

Synthesis and Biological Evaluation of the First Dual Tyrosyl-DNA Phosphodiesterase I (Tdp1)–Topoisomerase I (Top1) Inhibitors

Trung Xuan Nguyen,[†] Andrew Morrell,[†] Martin Conda-Sheridan,[†] Christophe Marchand,[‡] Keli Agama,[‡] Alun Bermingham,[§] Andrew G. Stephen,^{||} Adel Chergui,[‡] Alena Naumova,[‡] Robert Fisher,^{||} Barry R. O'Keefe,[§] Yves Pommier,[‡] and Mark Cushman^{*,†}

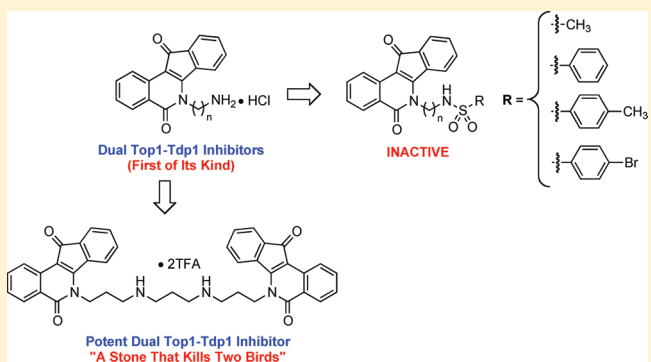
[†]Department of Medicinal Chemistry and Molecular Pharmacology, College of Pharmacy, and the Purdue Center for Cancer Research, Purdue University, West Lafayette, Indiana 47907, United States

[‡]Laboratory of Molecular Pharmacology, Center for Cancer Research, National Cancer Institute, Bethesda, Maryland 20892-4255, United States

[§]Molecular Targets Laboratory, Center for Cancer Research, National Cancer Institute, NCI-Frederick, Frederick, Maryland 21702, United States

^{||}Protein Chemistry Laboratory, Advanced Technology Program, SAIC-Frederick, Inc., NCI-Frederick, Frederick, Maryland 21702, United States

ABSTRACT: Substances with dual tyrosyl-DNA phosphodiesterase I–topoisomerase I inhibitory activity in one low molecular weight compound would constitute a unique class of anticancer agents that could potentially have significant advantages over drugs that work against the individual enzymes. The present study demonstrates the successful synthesis and evaluation of the first dual Top1–Tdp1 inhibitors, which are based on the indenoisoquinoline chemotype. One bis(indenoisoquinoline) had significant activity against human Tdp1 ($IC_{50} = 1.52 \pm 0.05 \mu M$), and it was also equipotent to camptothecin as a Top1 inhibitor. Significant insights into enzyme–drug interactions were gained via structure–activity relationship studies of the series. The present results also document the failure of the previously reported sulfonyl ester pharmacophore to confer Tdp1 inhibition in this indenoisoquinoline class of inhibitors even though it was demonstrated to work well for the steroid NSC 88915 (7). The current study will facilitate future efforts to optimize dual Top1–Tdp1 inhibitors.



INTRODUCTION

Eukaryotic topoisomerase I (Top1) is an essential enzyme for many critical cellular processes as it relaxes the double-helix structure of DNA so that the stored genetic information can be accessed during DNA replication, transcription, and repair.^{1,2} The mechanism of action of Top1 starts with the nucleophilic attack of the enzyme Tyr723 hydroxyl group on a phosphodiester linkage in DNA, displacing the 5'-end to become covalently attached to the 3'-end of DNA, thus forming a "cleavage complex."^{2,3} The religation reaction occurs faster than cleavage so the equilibrium favors the uncleaved DNA (Scheme 1).³

Under normal circumstances, the Top1–DNA cleavage complex is a transitory intermediate in the Top1-catalyzed reaction, as the broken DNA strand is quickly religated after a local supercoil has been removed.^{1–3} However, Top1 can become stalled in the DNA cleavage complex under a variety of natural or unnatural conditions in which the rate of religation is inhibited or reduced.^{4,5} For example, Top1 inhibitors, such as camptothecin (CPT, **1**) and its clinically used derivatives

(topotecan (**2**), irinotecan (**3**), and belotecan), as well as other non-CPT Top1 inhibitors like indenoisoquinolines (indotecan (**4**), and indimitecan (**5**)) (Figure 1), inhibit the religation rate by selectively and reversibly binding to the Top1–DNA interface.⁶ This ultimately leads to cell death after collision of the cleavage complex, with the replication fork resulting in double-strand breakage.^{7–9} Other naturally occurring DNA lesions, such as strand breaks, abasic sites, base mismatches, and certain oxidized or modified bases, can also induce stalled Top1–DNA complexes via the misalignment of the 5'-hydroxyl with the tyrosyl-DNA phosphodiester linkage, thus physically blocking the Top1 religation reaction.^{10,11} Under these conditions, cellular DNA metabolism results in repair of the stalled Top1–DNA cleavage complex by DNA ligase, which cannot work until the protein adduct is removed, and the broken DNA strand is provided with termini consisting of a 5'-phosphate on one end and a 3'-hydroxyl on the other for

Received: March 9, 2012

Published: April 26, 2012

Scheme 1. Top1 in Action

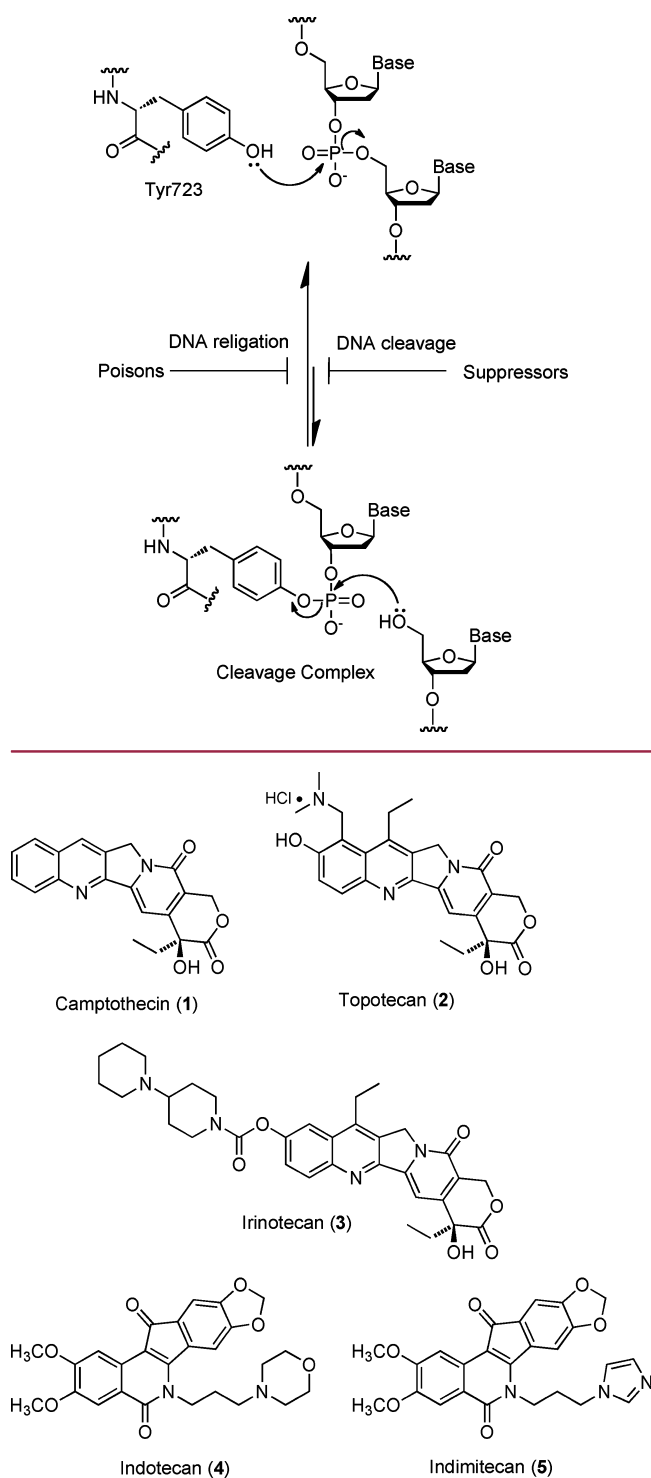


Figure 1. Representative Top1 inhibitors.

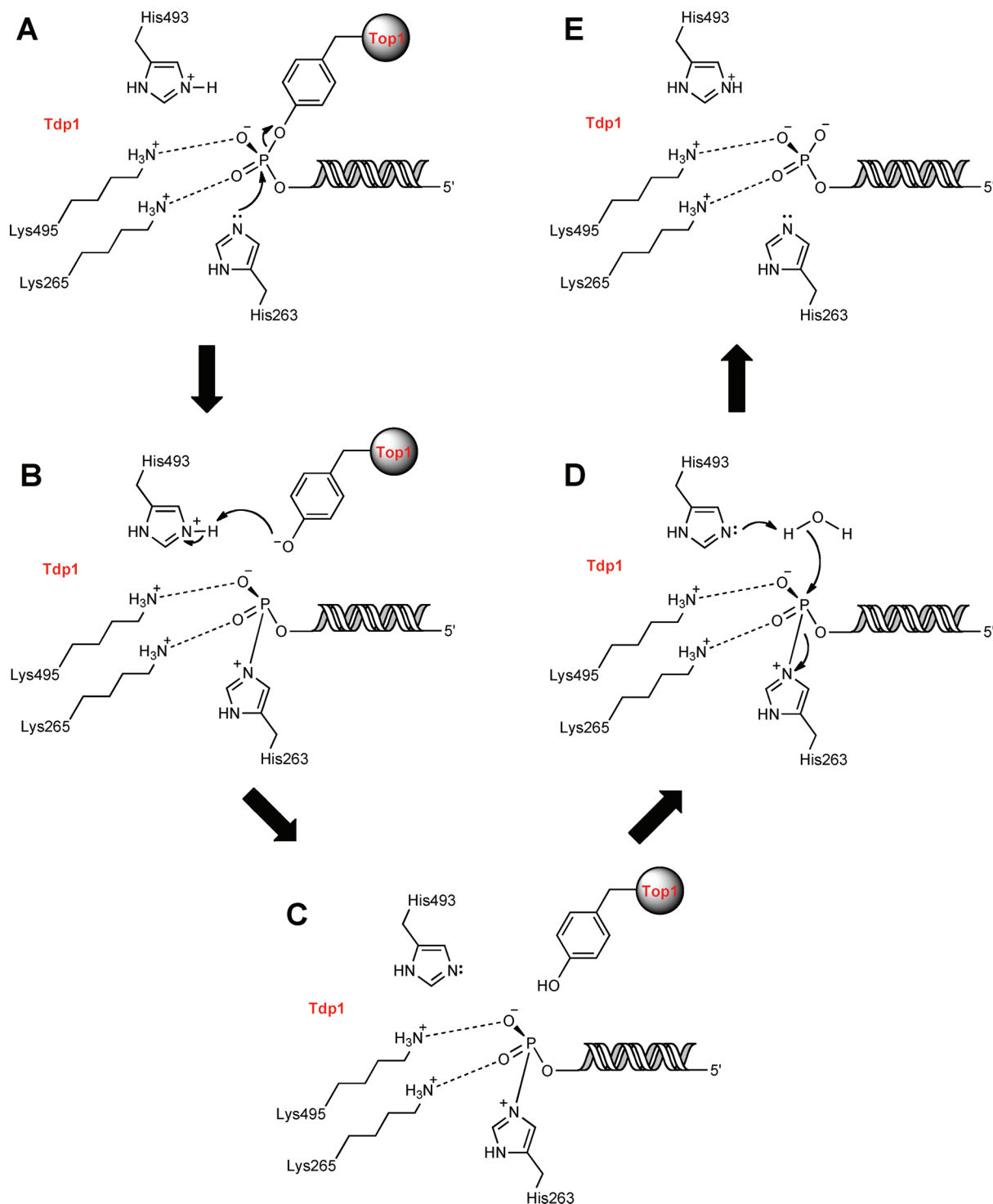
DNA repair.¹² In detail, the overall process involves the following steps: (1) tyrosyl-DNA phosphodiesterase I (Tdp1) hydrolyzes the phosphotyrosyl linkage between degraded Top1 and DNA, (2) polynucleotide kinase phosphatase (PNKP) hydrolyzes the resulting 3'-phosphate end and catalyzes the phosphorylation of the 5'-hydroxyl end of the broken DNA strand. This results in a broken DNA strand with termini consisting of a 5'-phosphate and 3'-hydroxyl for DNA repair.

(3) DNA polymerase β replaces the missing DNA segment, and finally, (4) DNA ligase III reseals the broken DNA.¹²

Tyrosyl-DNA phosphodiesterase I (Tdp1) has been shown to be the only enzyme that specifically catalyzes the hydrolysis of the phosphodiester bond between the catalytic Tyr723 of Top1 and DNA-3'-phosphate.¹³ Hence, Tdp1 is thought to be associated with the repair of DNA lesions. The cellular importance of Tdp1 also stems from the fact that it is ubiquitous in eukaryotes and plays an important physiological role, as the homozygous mutation H493R in its active site is responsible for the rare autosomal recessive neurodegenerative disease called spinocerebellar ataxia with axonal neuropathy (SCAN1).¹⁴ Tdp1 also has the ability to remove the 3'-phosphoglycolate caused by oxidative DNA damage by bleomycin¹⁵ and repair trapped Top2-DNA cleavage complexes.^{16,17} All this evidence suggests that Tdp1 assumes a broader role in the maintenance of genomic stability. Hence, this makes Tdp1 a rational anticancer drug development target.^{12,18}

Tdp1 is a member of the phospholipase D superfamily of enzymes that catalyze the hydrolysis of a variety of phosphodiester bonds in many different substrates.¹⁹ Crystallographic studies have revealed that human Tdp1 is composed of two domains related by a pseudo-2-fold axis of symmetry.²⁰ Each domain contributes a histidine and a lysine residue to form an active site that is centrally located at the symmetry axis.²⁰ Four additional residues, N283, Q294, N516, and E538, are also positioned near the active site.²⁰ The crystal structure of Tdp1 in the quaternary complex with a vanadate ion, a Top1-derived peptide, and a single-stranded DNA oligonucleotide revealed an active site in which the DNA moiety occupies a relatively narrow cleft rich in positive charges, while the peptide moiety binds in another region of the active site characterized by a relatively large, more open cleft that contains a mixed charge distribution.²⁰⁻²² The trigonal bipyramidal geometry exhibited by the vanadate implies an S_N2 mechanism for nucleophilic attack on phosphate.^{21,22} Therefore, the mechanism of action of Tdp1 is proposed to start with a nucleophilic attack on the phosphotyrosyl bond by the catalytic H263 residue in the N-terminal domain, while the H493 residue in the C-terminal domain acts as a general acid and donates a proton to the tyrosine-containing peptide leaving group (Scheme 2).²¹ The resulting phosphoramidate is stabilized by hydrogen-bonding with catalytic K265 and K495. Hydrolysis of this covalent intermediate occurs via a second S_N2 reaction by a water molecule with the H493 residue acting as a general base.²¹ This proposed reaction step is supported by *in vitro* studies showing that the SCAN1 H493R mutation leads to an accumulation of Tdp1-DNA covalent intermediate.²³ The final product in this process is a DNA molecule with a 3'-phosphate end.¹²

Because the Top1-DNA phosphotyrosyl bond is buried deep within the Top1-DNA complex and is inaccessible to Tdp1,²⁴ prior denaturation of the Top1-DNA complex or proteolytic degradation of Top1 is required for the Tdp1 enzymatic activity.^{25,26} However, Tdp1 seems to be equally effective against many structural variations of DNA, including single-strand, tailed duplex, and gapped duplex,^{12,27,28} although the activity decreases as the oligonucleotide length is shortened.^{12,25} These observations have implied that the enzymatic activity of Tdp1 is influenced by the length of Top1-derived polypeptide chain and the structure of the DNA segment bound to Top1.^{25,26} Moreover, studies from SCAN1

Scheme 2. Tdp1 in Action¹²

cells provided evidence for Tdp1 participation in the repair of Top1-mediated DNA damage^{23,29,30} and for the hypersensitivity to camptothecin in human cells with a single defect in Tdp1 activity.^{15,31} These observations suggest the possibility of developing Tdp1 inhibitors that can potentiate the cytotoxic effects of Top1 inhibitors in anticancer drug therapy.¹²

To date, there are very few known Tdp1 inhibitors, and their potencies and specificities leave much room for improvement (Figure 2). For example, both vanadate and tungstate can mimic the phosphate in the transition state, thus expressing

inhibition at millimolar concentrations.^{20,21} However, due to poor specificity and hypersensitivity to all phosphoryl transfer reactions, they cannot serve as pharmacological inhibitors.¹² Other Tdp1 inhibitors are the aminoglycoside neomycin, which has very low potency at $IC_{50} = 8 \text{ mM}$,³² or furamidine (**6**), which produces reversible and competitive inhibition of Tdp1 with an $IC_{50} \approx 30 \mu\text{M}$.³³ However, **6** has additional targets because of its DNA binding activities, which also makes experimental data difficult to interpret.³³ The steroid NSC 88915 (**7**) was recently identified via high-throughput screening

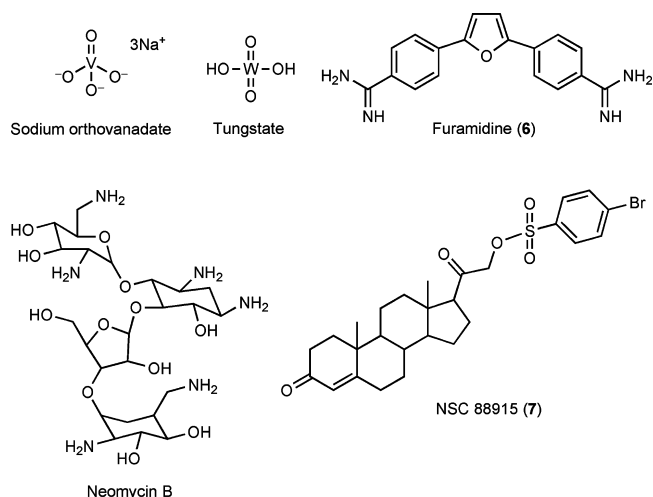


Figure 2. Representative Tdp1 inhibitors.

as a potent and specific Tdp1 inhibitor with an $\text{IC}_{50} = 7.7 \mu\text{M}$.³⁴ However, this compound expressed some common pharmacokinetic problems in cellular systems such as limited drug uptake, poor cytotoxicity, and off-target effects.³⁴ Therefore, there is an urgent need to design and develop potent Tdp1 inhibitors that can overcome these drawbacks. Furthermore, potential anticancer agents that would possess both Tdp1 and Top1 inhibitory activities are attractive because the two types of activities could act synergistically.

TDP1 INHIBITOR DISCOVERY AND OPTIMIZATION

Screening of a focused library of indenoisoquinolines led to the discovery of three potent Tdp1 inhibitors (Table 1). These

Table 1. Tdp1 Inhibitory Activities of *n*-Alkylamino Indenoisoquinolines



Compound 77-79

<i>n</i>	IC_{50} (μM) recombinant Tdp1	α^{Top1}
10	14	0
11	13	+
12	15	0/+

^aCompound-induced DNA cleavage due to Top1 inhibition is graded by the following semiquantitative scale relative to $1 \mu\text{M}$ camptothecin (1): 0, no inhibitory activity; +, between 20 and 50% activity; ++, between 50 and 75% activity; +++, between 75% and 95% activity; ++, equipotent. The 0/+ ranking is between 0 and +.

Tdp1-active *n*-alkylamino-containing indenoisoquinolines 77–79 ($n = 10$ – 12), which had been synthesized previously by Morrell et al.,³⁵ did not display Top1 inhibition or were very weak inhibitors, although other homologous compounds with shorter linkers (69–71, $n = 2$ – 4) were good Top1 inhibitors.³⁶ This led to the idea that Tdp1 inhibition may potentially be present in Top1 inhibitors with a shorter side chain. In

addition, previous studies reported the importance of the sulfonate functional group in conferring the Tdp1 inhibitory activity of steroid 7 (Figure 2) because this group mimics the phosphotyrosyl bond in the Top1–DNA complex.³⁴ This led to the hypothesis that sulfonate analogues of the indenoisoquinolines in Table 1 might function as Tdp1 inhibitors. This hypothesis was also supported by GOLD docking and energy minimization of one hypothetical sulfonate (25, $n = 3$) in the crystal structure of Tdp1 (1RFF) after deleting the polydeoxyribonucleotide 5'-D(*AP*GP*TP*T)-3', vanadate (VO_4^{3-}), and the Top1-derived peptide residues 720–727 (mutation L724Y). The docking results revealed a structure that resembles the original structure: the tosylate moiety matched the phosphotyrosine, the sulfonate was in place of the vanadate, the alkyl chain played the “spacer” role of the deoxyribose, and the indenoisoquinoline system overlapped with a thymine of DNA (Figure 3). This result is in agreement with those reported for steroid 7.³⁴ Because a sulfonamide bond is well-known to be more metabolically stable than a sulfonate and the current compounds possess a structural handle (amino group) that can be used to install a sulfonyl linkage, a series of indenoisoquinoline sulfonates and sulfonamides with different linker lengths ($n = 2$ – 12) were synthesized in order to investigate how the structures of these indenoisoquinolines resemble the substrate of the Tdp1-catalyzed reaction. Moreover, a previous study on steroid 7 indicated that different substituents on the phenyl ring may have positive effects on Tdp1 inhibitory activity.³⁴ Therefore, four different groups were placed at the sulfonamide position (Figure 4).

The ultimate goal of this project was to design and synthesize compounds with dual Top1–Tdp1 inhibitory activities. Recent studies have provided some evidence for a potential DNA interaction of Tdp1 inhibitors.^{19,34} Prior studies demonstrated that bis(indenoisoquinolines) monointercalate with DNA and inhibit the DNA religation reaction by intercalating between base pairs at the cleavage site in the ternary Top1–DNA–drug cleavage complex.³⁷ This led to the consideration of bis-(indenoisoquinolines) as possible Tdp1 inhibitors. Figure 4 shows a summary of compounds proposed for synthesis.

CHEMISTRY

Synthesis of Indenoisoquinoline Sulfonates. The key starting material in the synthesis of all of the desired compounds is lactone 11, which was synthesized based on the procedure reported by Morrell et al.³⁸ The reaction of 2-carboxybenzaldehyde (8) and phthalide (9) in the presence of sodium methoxide in methanol yielded the intermediate 10, which formed lactone 11 upon cyclization under acidic conditions in a one-pot synthesis carried out with the aid of a Dean–Stark trap. The synthetic route to indenoisoquinoline sulfonates 24–29 involved the preparation of *n*-hydroxyalkyl indenoisoquinolines 18–23 from the reaction of lactone 11 and *n*-aminoalcohols 12–17 for 3–6 h. The sulfonylation of compounds 19–23 to afford indenoisoquinoline sulfonates 25–29 was achieved in dichloromethane (Scheme 3).

However, the sulfonylation of 2-hydroxyethyl indenoisoquinoline 18 under the same conditions failed to yield the desired sulfonate product 24 but instead gave the chloride analogue 30 or, in the presence of silver acetate, the acetate analogue 31 (Scheme 4). Silver acetate was initially meant to quench the nucleophilic attack of the chloride ions in the hope of obtaining the sulfonate 24, and the side product 31 was unexpected.

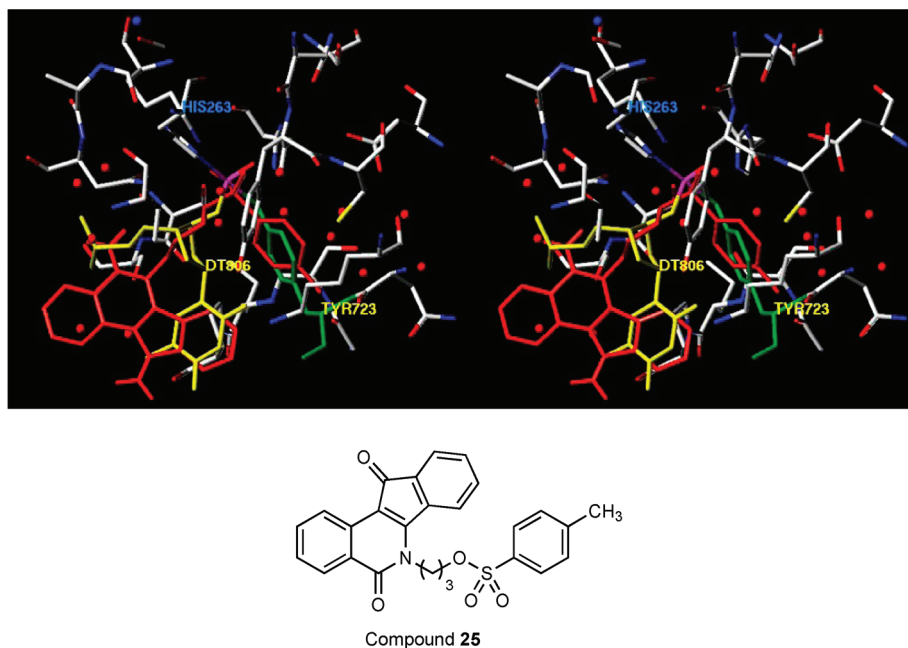


Figure 3. Overlapped hypothetical structures of the binary complex Tdp1–indenoisoquinoline sulfonate 25 and the crystal structure of the quaternary complex consisting of Tdp1–5'-D(*AP*GP*TP*T)-vanadate-3'-Top1-derived peptide residues 720–727 (mutation L724Y).³⁶ Red, indenoisoquinoline sulfonate; green, Tyr723; yellow, DT806; vanadate, fuchsia. The figure is programmed for wall-eyed (relaxed) viewing.

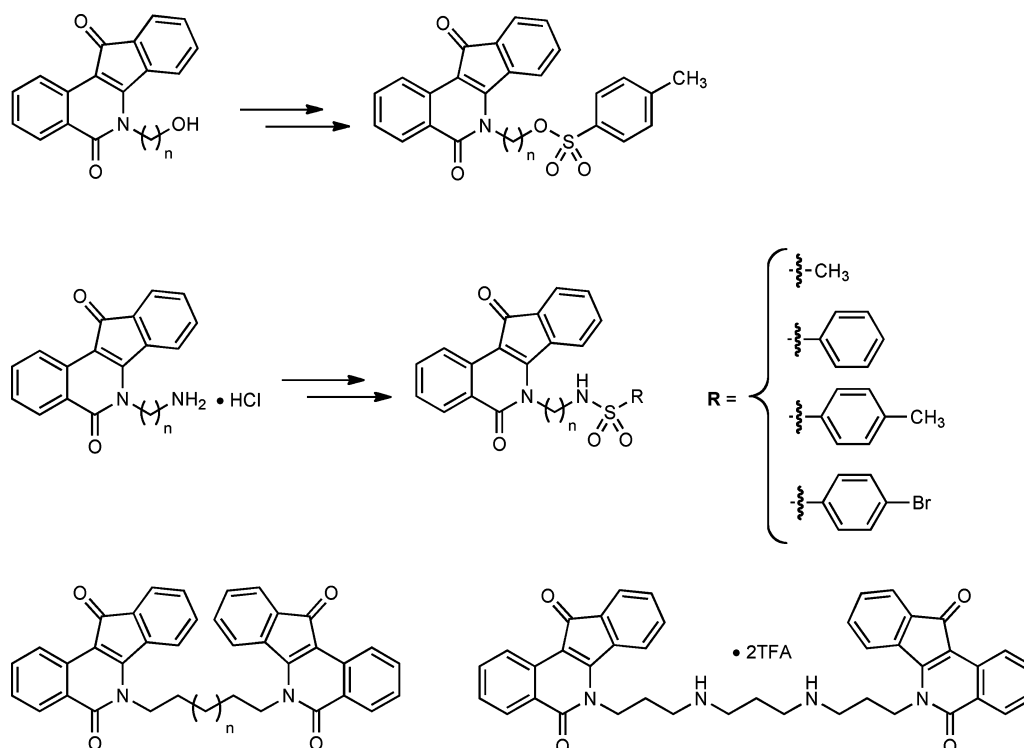
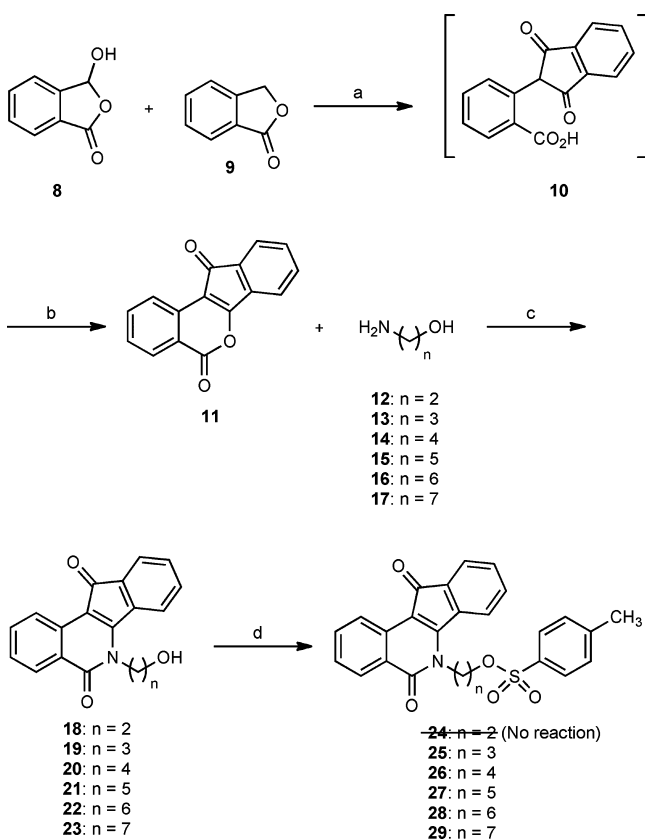


Figure 4. Compounds proposed for synthesis.

Two mechanisms are proposed for this transformation with the sulfonate 24 assumed to be the first intermediate (Scheme 5). In the first proposed mechanism, 24 undergoes intramolecular cyclization and elimination of the tosylate group to yield a 4,5-dihydro-3-oxazolium intermediate 32. Nucleophilic attack of the chloride anion yields the substituted 2-chloroethyl indenoisoquinoline 30. The presence of silver ion facilitates the displacement of chloride by acetate to form 31. In the second

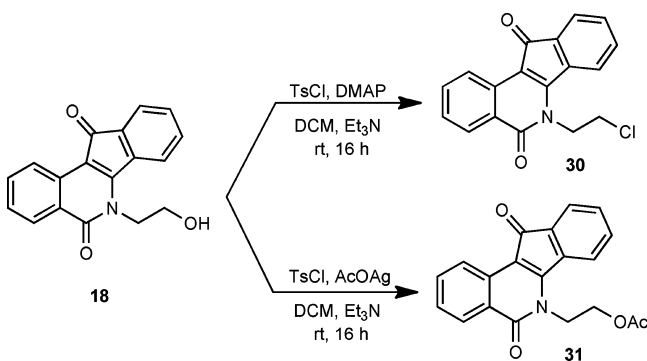
mechanism, chloride displaces the tosylate directly to form 31. This mechanism does not explain why the alcohol 18 undergoes a unique reaction pathway.

An independent study of the feasibility of displacing the chloride by acetate was done by mixing and stirring chloride 30 and silver acetate in dichloromethane without the presence of any base at room temperature for 24 h. The result showed that 30 was incompletely converted to the acetate 31 and,

Scheme 3. Synthesis of Indenoisoquinoline Sulfonates^a

^aReagents and conditions: (a) NaOMe, MeOH, EtOAc, 65 °C; (b) HCl, PTSA, benzene, reflux; (c) CHCl₃, reflux; (d) TsCl, DMAP, CH₂Cl₂, Et₃N, rt.

Scheme 4. Formation of the Undesired Chloride (30) and Acetate (31) Analogues



surprisingly, to alcohol 18. This result implied the sensitivity of acetate 31 to hydrolysis and its instability in solution.

7-Hydroxyheptyl indenoisoquinoline 23 could be prepared from lactone 11 and the commercially available 7-amino-1-heptanol (17) as depicted in Scheme 3. However, due to the very high cost of 17 (and any *n*-aminoalcohol with more than six methylene units), several alternative routes were considered for making 23. Aminoalcohol 17 can be readily prepared from the reaction of its low-cost 7-bromo analogue 33 with sodium azide in CHCl₃ to afford an azido intermediate, which yields 17 upon reduction with Fe in aqueous ammonia (Scheme 6A). However, because this route poses an explosion hazard due to the instability of the azido compound and the possible

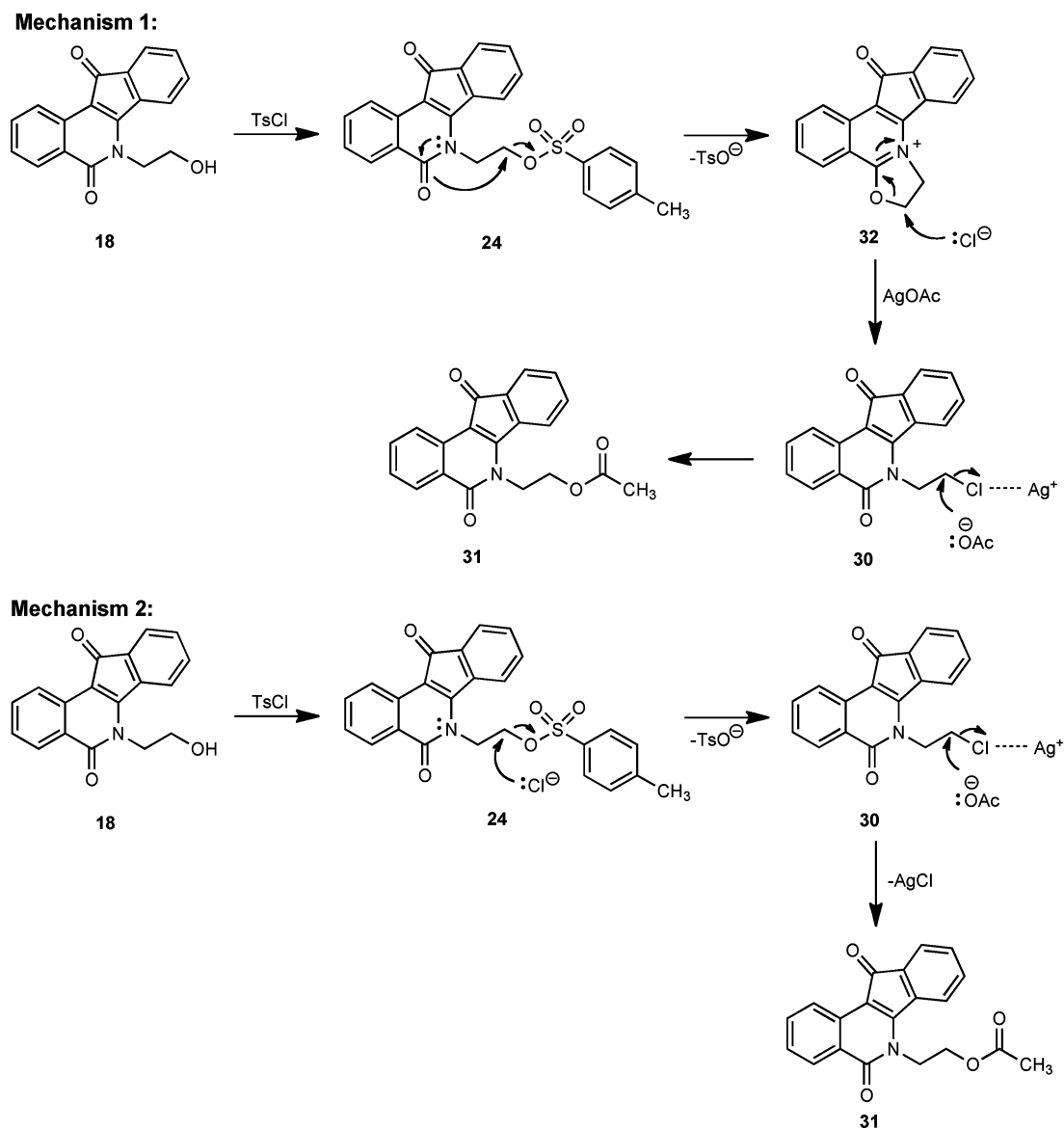
formation of the very explosive di- and triazidomethane (from CHCl₃) during workup,³⁹ an alternative route was utilized to make 17 under safer and milder conditions using the classical Delépine reaction (Scheme 6B). In this method, urotropine 34 was alkylated by the 7-bromoalcohol 33 to produce a quaternary hexamethylenetetramine salt 35, which produced the 7-aminoalcohol 17 in good yield upon acidic hydrolysis in ethanol. Another advantage of this method is that intermediate 17 requires no purification and can react with lactone 11 to afford 23 in very high purity.

Synthesis of Indenoisoquinoline Sulfonamides. All the desired *n*-alkylamino indenoisoquinoline hydrochloride salts 69–79 were synthesized based on the procedures reported by Morrell et al.³⁵ as follows: the diamines 36–46 were Boc protected at one end by using a 5:1 diamine:Boc₂O ratio. The mono-Boc-protected products 47–57 were treated with lactone 11 in a 1:1 ratio to give the Boc-protected indenoisoquinolines 58–68 in high yields, which, upon deprotection of the amines in methanolic HCl, provided the indenoisoquinoline hydrochloride salts 69–79. All of the indenoisoquinoline sulfonamides with methyl (80–90), phenyl (91–101), *p*-methylphenyl (102–112), and *p*-bromophenyl (113–123) substituents were synthesized in good to excellent yields by gently heating each hydrochloride salt at 70 °C with a corresponding sulfonating reagent (mesyl, benzenesulfonyl, tosyl, or *p*-bromobenzenesulfonyl chloride) in 1:2 ratio in the presence of triethylamine (2 equiv) for 16 h (Scheme 7).

A different synthetic route to the indenoisoquinoline sulfonamides was investigated as follows: (1) the sulfonamide group was incorporated into the linker chain by having the sulfonating reagents (mesyl, benzenesulfonyl, tosyl, or *p*-bromobenzenesulfonyl chloride) react with diamines in a 1:5 molar ratio, with the procedure for these reactions being similar to that of making mono-Boc-protected diamines, (2) heating the monosulfonated diamines with lactone 11 in a 1:1 molar ratio under reflux to obtain the desired sulfonamides (Scheme 8). The advantage of this approach is that the introduction and removal of the protecting Boc group were skipped, thus providing a shorter route to make sulfonamides with hypothetically higher overall yields. However, the apparent weakness is that derivatization of side chains at the sulfonamide end would be impossible. Nevertheless, this idea was first tested by the reaction of *N*-(3-aminopropyl)-4-methylbenzenesulfonamide (124) with lactone 11 to give sulfonamide 103 in 70% yield. Following this success, *N*-(11-aminoundecyl)-4-methylbenzenesulfonamide (125) and *N*-(11-aminoundecyl)-benzenesulfonamide (126) were synthesized to use in the next reaction with lactone 11. However, the condensation occurred very slowly in CHCl₃ and a significant amount of starting materials was observed even after 48 h of heating at reflux. Then benzene was employed to help remove H₂O from the reaction mixture in order to force the equilibrium to the product side, but the reaction provided only about 30% yield of crude product after 2 days of heating in the presence of a Dean–Stark trap and starting materials were still present in the mixture. Hence, the original method was utilized to make all of the desired sulfonamides 80–123.

Synthesis of Bisindenoisoquinolines and Other Compounds. The goal of this project was to achieve dual Top1–Tdp1 inhibition, and this was attempted by making sulfonamides from substrates that have been shown to be active against Top1 by previous biological assays (Figure 5).⁴⁰ The presence of a bulky substituent at position 9 on the D-ring

Scheme 5. Proposed Mechanisms for the Formation of Chloride 30 and Acetate 31



of the indenoisoquinoline system attenuates Top1 inhibition,⁴⁰ as seen in compounds **127** and **129** (see structure **127** in Figure 5 for indenoisoquinoline numbering). Nevertheless, to gain a quick look into the effects of various substituents on the A- and D-rings of the indenoisoquinoline system to Tdp1 inhibitory activity, all the starting materials **127**–**131** were subjected to similar reaction conditions to obtain the corresponding sulfonamides **132**–**136** (Figure 5). In addition, three bis-(indenoisoquinolines) **140**–**142** were prepared by heating 2 equiv of lactone **11** with diamines **137**–**139** at reflux for 16 h. Polyamino bis(indenoisoquinoline) **145** was synthesized based on the procedure reported by Morrell et al.³⁷ (Scheme 9).

■ BIOLOGICAL RESULTS AND DISCUSSION

Tdp1 inhibitory activity was measured by the drug's ability to inhibit the hydrolysis of the phosphodiester linkage between tyrosine and the 3'-end of the DNA substrate and to prevent the generation of an oligonucleotide with a free 3'-phosphate (N14P).³⁴ Therefore, the disappearance of the gel band for N14P indicated Tdp1 inhibition. The Tdp1 catalytic gel-based

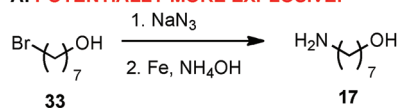
assay is represented in Figure 6, and representative gels demonstrating dose-dependent Tdp1 inhibition by some indenoisoquinoline amine hydrochlorides are depicted in Figure 7.

Additionally, all indenoisoquinoline sulfonates and sulfonamides were tested for Top1 cleavage complex poisoning in a Top1-mediated DNA cleavage assay.⁴¹ The potency of a compound against Top1 is correlated to the intensities of the bands corresponding to DNA fragments in this assay and is graded by the following semiquantitative scale relative to 1 μ M camptothecin: 0, no inhibitory activity; +, between 20% and 50% activity; ++, between 50% and 75% activity; +++, between 75% and 95% activity; +++++, equipotent. The Tdp1 and Top1 activities of all target compounds are represented in Figure 8.

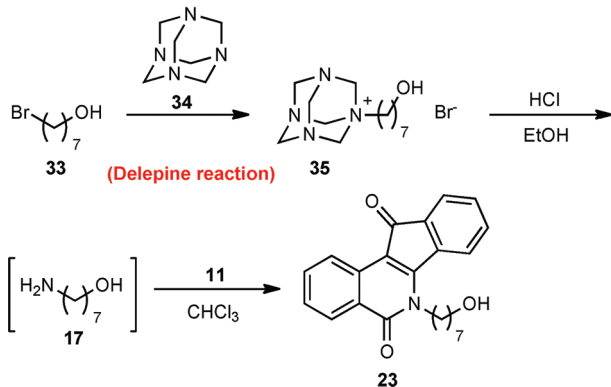
The indenoisoquinoline amine hydrochlorides **69**–**79** were shown to be Tdp1 inhibitors (IC_{50} = 13 to 55 μ M). Despite being less active than steroid **7** (Figure 2, IC_{50} = 7.7 μ M), their potencies were retained in whole cell extract while the steroid expressed off-target effects and lost its potency in cellular environments.³⁴ Notably, compounds with longer linkers (n = 10–12) showed higher Tdp1 inhibition than those with shorter

Scheme 6. Alternative Routes to Synthesize 17

A. POTENTIALLY MORE EXPLOSIVE!



B. SAFER & GREENER



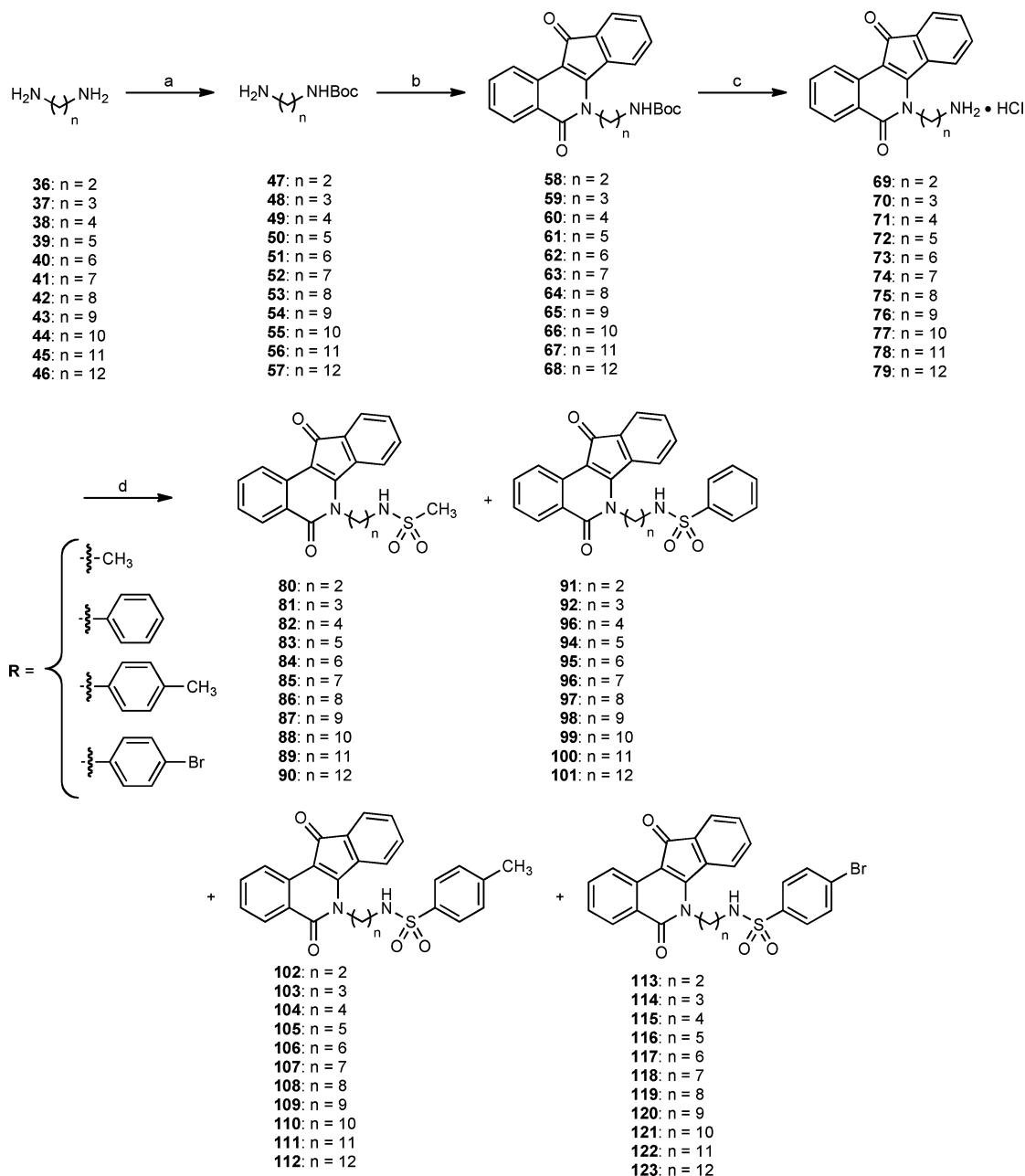
side chains, while the Top1 inhibition trend was the opposite. It is known that the optimal length of the side chain at the lactam position in Top1 indenoisoquinoline inhibitors is three methylene units (propyl).^{35,40} Molecular modeling indicated that an increase in hydrophobicity as a direct result of increased linker length in these Top1 inhibitors caused negative interactions with the hydrated binding pocket of the Top1–DNA cleavage complex.³⁵ That explained the decrease in Top1 inhibition of this series as the number of methylene units increases. This is, however, not the case for Tdp1 inhibition. Although the present results for Tdp1 inhibition do not show a linear correlation of chain length and potency, they indicate that the longer chains may gain favorable hydrophobic interactions in the binding site of Tdp1. Additionally, hypothetical models show that the lactam side chain protrudes toward the major groove of DNA and causes minimal steric clashes within the binding pocket in the Top1–DNA cleavage complex.³⁵ Similar conclusions can be drawn for Tdp1: because no significant reduction in activity was observed in the series with increasing chain length, the lactam side chain must be well accommodated. Indenoisoquinolines with $n = 3$ and 4 (compounds 70 and 71) with $IC_{50} = 22\text{--}29\ \mu\text{M}$, $MGM\ GI_{50} = 0.16\text{--}0.32\ \mu\text{M}$,³⁵ Top1 inhibition “+++” are the most potent representatives of the 69–79 series tested for dual Top1–Tdp1 inhibitory activity. These also represent a new chemotype of fully synthetic small-molecule Tdp1 inhibitors.

Surprisingly, the hydroxyl analogues (compound 18–23) were inactive against Tdp1. Despite being similar in ability to form hydrogen bonds, the discrepancy in Tdp1 potency when going from the amino group to the hydroxyl group in this series lends support to the hypothesis that hydrogen bonding may not be a predominant factor that determines Tdp1 inhibitory activity. Moreover, it seems reasonable to consider these amino inhibitors to be protonated at physiological pH, and this positively charged state, which is not possible in the hydroxyl series 18–23, seems to be an important requirement for Tdp1 inhibition. This rationale is in agreement with a previous report that the terminal amino group in this series is important for cellular cytotoxicity although not absolutely necessary for Top1 inhibition.³⁵

One member of this amino series (70, $n = 3$) was subjected to surface plasmon resonance (SPR) assays based on reported procedures³⁴ in order to gain a more detailed understanding of the Tdp1–inhibitor interaction and to measure the affinity of 70 to Tdp1 (Figure 9). The binding of the inhibitor to the surface-bound Tdp1 induces an increase in resonance units from the initial baseline until a steady-state phase of this interaction is achieved as depicted by a plateau.³⁴ The decrease in resonance units corresponds to the dissociation or reversibility of the interaction.³⁴ This result demonstrates direct binding of 70 to Tdp1. This compound was also evaluated using a fluorescence resonance energy transfer (FRET) assay and was found to be a competitive inhibitor with $K_i = 3.19\ \mu\text{M}$ (Figure 10). Steroid 7, which binds Tdp1 directly, is also competitive with the DNA substrate for the Tdp1 active site.³⁴

All indenoisoquinoline sulfonates and sulfonamides (compounds 80–123) were inactive against Tdp1 ($IC_{50} > 111\ \mu\text{M}$). This result was unexpected because extensive studies on steroid 7 clearly emphasized the importance of the sulfonyl ester moiety for Tdp1 inhibition,³⁴ and our initial modeling (Figure 3) also suggested a good mimic of the phosphotyrosine linkage by the sulfonate group, which is similar to how steroid 7 resembles this group. As the sulfonate or sulfonamide moiety was attached to the terminal amino group, the activity was completely abolished independently of the linker length ($n = 2\text{--}12$). Similarly, sulfonamides 132–136 were also inactive against Tdp1. Although steric clashes between the sulfonate or sulfonamide group with components of the binding pocket might be responsible for this result, this explanation is not satisfactory because even when a short side chain is present such as in compound 80, which bears a relatively small mesylate group on an ethyl linker, the activity drops drastically. In the case of the amino series (compounds 69–79), the ligand-binding site seems to accommodate a long side chain quite well. Therefore, steric clashes could only explain the inactivity of compounds with very long and bulky side chains. A different factor must have been the cause of the significant attenuation of Tdp1 inhibition upon sulfonylation of the amino series even though this was completely different in case of steroid 7. Because of the lack of a crystal structure of Tdp1 in complex with an inhibitor, no firm conclusion can be drawn as to where a ligand binds and how it inhibits Tdp1 activity, and molecular modeling failed to provide an answer to the question of sulfonate and sulfonamide inactivities in the present series.

Among the four bis(indenoisoquinolines) synthesized and tested, only the polyamino bis(indenoisoquinoline) 145 displayed low micromolar Tdp1 inhibition, with an $IC_{50} = 1.5\ \mu\text{M}$ and $1.9\ \mu\text{M}$ against rec and WCE Tdp1, respectively. Three other bis(indenoisoquinolines) 140–142, which were made because of the initial positive results from the amino series with 10–12 methylene linkers, were inactive. This result provides additional support to the hypothesis that the protonation of the amino groups may give favorable charge-complementary interactions within the Tdp1 binding pocket, thereby conferring Tdp1 inhibition. The polyamino bis(indenoisoquinoline) 145 is currently the most potent dual Top1–Tdp1 inhibitor, displaying Top1 inhibition (“++++”) equipotent to camptothecin,³⁷ excellent antiproliferative potency ($MGM\ GI_{50} = 0.394\ \mu\text{M}$),³⁷ and also excellent inhibitory activity against Tdp1 in both human rec. and WCE Tdp1 with $IC_{50} = 1.5$ and $1.9\ \mu\text{M}$, respectively.

Scheme 7. Synthesis of Indenoisoquinoline Sulfonamides^a

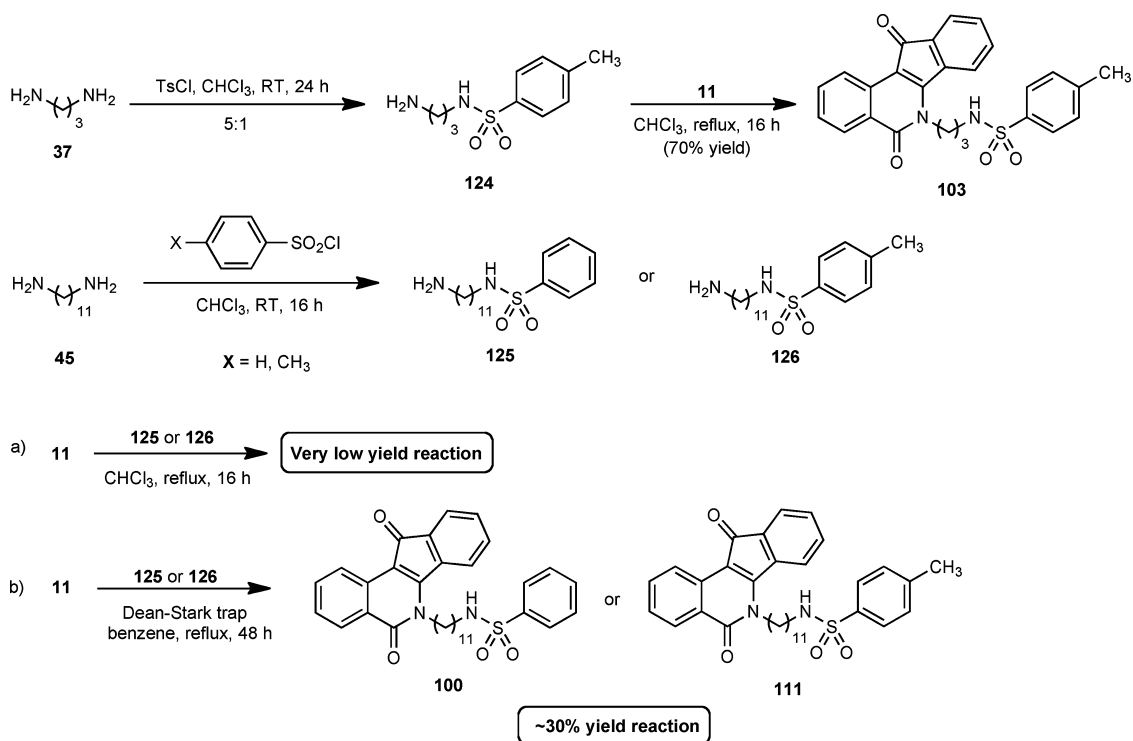
^aReagents and conditions: (a) Boc₂O, CHCl₃, rt; (b) **11**, CHCl₃, reflux; (c) 3 M HCl in MeOH, rt; (d) RSO₂Cl, Et₃N, CHCl₃, 70 °C.

CONCLUSION

A series of bis(indenoisoquinolines) and indenoisoquinolines with amino, sulfonate, and sulfonamide side chains have been synthesized to evaluate the hypothesis that dual Top1–Tdp1 inhibition can be achieved in a single compound. In contrast with the reported importance of the sulfonyl ester moiety to the Tdp1 inhibition, all sulfonates and sulfonamides were inactive while the free amines at various linker lengths displayed good to excellent inhibition. Among them, two compounds, **70** and **71**, were potent against both Tdp1 and Top1, and the overall series represents the first dual Top1–Tdp1 inhibitors ever reported. Significant insights for future lead optimization were deduced: (1) hypothetical charge-complementary interactions between protonated amino groups within the Tdp1 active site may contribute to high potency, and (2) the hydrophobicity of

the polymethylene moiety linking the amino group to the heterocycle may also contribute to activity. The polyamino bis(indenoisoquinoline) **145** is currently the most potent dual Top1–Tdp1 inhibitor. This encouraging result has much significance because: (1) this class of indenoisoquinoline compounds serves as the first evidence that having Top1 and Tdp1 inhibitory activity in one single small molecule is in fact possible, (2) the unique structural features of indenoisoquinolines allow much room for manipulation so the pharmacokinetics (absorption, distribution, and excretion) can be modulated and optimized in ways that are not possible for other types of Tdp1 inhibitors, (3) they represent lead molecules for development of new dual Top1–Tdp1 inhibitory agents, and (4) they provide a set of inhibitory ligands that

Scheme 8. Alternative Synthetic Route to Indenoisoquinoline Sulfonamides



could possibly be crystallized in complex with Tdp1, which would facilitate the structure-based drug design approach.

EXPERIMENTAL SECTION

General. Solvents and reagents were purchased from commercial vendors and were used without any further purification. Melting points were determined using capillary tubes with a Mel-Temp apparatus and were uncorrected. Infrared spectra were obtained using KBr pellets using CHCl₃ as the solvent. IR spectra were recorded using a Perkin-Elmer 1600 series or Spectrum One FTIR spectrometer. ¹H NMR spectra were recorded at 300 MHz using a Bruker ARX300 spectrometer with a QNP probe. Mass spectral analyses were performed at the Purdue University Campus-Wide Mass Spectrometry Center. ESI-MS studies were performed using a FinniganMAT LCQ Classic mass spectrometer. EI/CI-MS studies were performed using a Hewlett-Packard Engine or GCQ FinniganMAT mass spectrometer. APCI-MS studies were carried out using an Agilent 6320 ion trap mass spectrometer. Combustion microanalyses were performed at Midwest Microlab, LLC. All reported values are within 0.4% of the calculated values. Analytical thin layer chromatography was carried out on Bakerflex silica gel IB2-F plates, and compounds were visualized with short wavelength UV light and ninhydrin staining. Silica gel flash chromatography was performed using 230–400 mesh silica gel. HPLC analyses were performed on a Waters 1525 binary HPLC pump/Waters 2487 dual λ absorbance detector system using a 5 μ M C₁₈ reverse phase column. Purities of biologically important compounds were \geq 95%. For purities estimated by HPLC, the major peak accounted for \geq 95% of the combined total peak area when monitored by a UV detector at 254 nm. All yields refer to isolated compounds.

Benz[*d*]indeno[1,2-*b*]pyran-5,11-dione (11).³⁸ Sodium metal (3.678 g, 0.160 mol) was cut into small pieces and added to MeOH (40 mL) to make a 4 M methanolic solution of sodium methoxide, which was then added to a solution of 2-carboxybenzaldehyde (8) (1.000 g, 6.661 mmol) and phthalide (9) (0.893 g, 6.661 mmol) in ethyl acetate (20 mL). The mixture was stirred and heated at 70 °C for 16 h to yield an orange solution, which was then concentrated, diluted with H₂O (100 mL), acidified with 10% HCl until pH 1, and extracted

with EtOAc (50 mL \times 3). The organic layers were combined and extracted with 1 N NaOH (50 mL \times 3). The aqueous layers were combined and acidified with concentrated HCl until pH 1 to give a red solution. The acidic mixture was extracted with ethyl acetate (50 mL \times 3) and washed with brine (50 mL). The organic layers were dried over anhydrous MgSO₄, filtered, and concentrated to yield the intermediate 10. The crude intermediate 10 was dissolved in benzene (125 mL), followed by an addition of TsOH·H₂O (100 mg). The resulting mixture was heated for 7 h at reflux in a flask affixed with a Dean-Stark trap. The solution was cooled to room temperature, concentrated, diluted with CHCl₃ (150 mL), and washed with satd NaHCO₃ (50 mL \times 3) and brine (50 mL). The organic layer was dried over anhydrous Na₂SO₄ and concentrated to yield the desired product as an orange solid (1.69 g, 93%); mp 254–256 °C (lit.³⁸ 257 °C). ¹H NMR (300 MHz, CDCl₃) δ 8.39 (d, *J* = 7.8 Hz, 1 H), 8.31 (d, *J* = 8.2 Hz, 1 H), 7.84 (t, *J* = 7.5 Hz, 1 H), 7.61 (d, *J* = 6.9 Hz, 1 H), 7.55–7.39 (m, 4 H).

General Procedure for the Preparation of *n*-Hydroxyalkyl Indenoisoquinolines 18–22. *n*-Aminoalcohols 12–16 (0.50 g) in CHCl₃ (10 mL) were added to a solution of lactone 11 (1.0 equiv) in CHCl₃ (50 mL). The reaction mixtures were heated at reflux for 3–6 h with stirring and then washed with H₂O (50 mL \times 2) and brine (50 mL). The organic layers were dried over anhydrous Na₂SO₄, filtered, and concentrated, adsorbed onto SiO₂, and purified by flash column chromatography (SiO₂), eluting with 5% MeOH in CHCl₃, to provide the products 18–22 in high purity.

6-(2-Hydroxyethyl)-5*H*-indeno[1,2-*c*]isoquinoline-5,11(6*H*)-dione (18).⁴² The general procedure provided the desired product as a red solid (1.10 g, 62%); mp 201–204 °C (lit.⁴² 200–201 °C). ¹H NMR (300 MHz, CDCl₃) δ 8.68 (d, *J* = 8.1 Hz, 1 H), 8.32 (d, *J* = 8.3 Hz, 1 H), 7.74 (dt, *J* = 1.2 and 7.1 Hz, 1 H), 7.62 (dd, *J* = 1.2 and 7.0 Hz, 2 H), 7.48–7.37 (m, 3 H), 4.76 (t, *J* = 5.8 Hz, 2 H), 4.21 (q, *J* = 5.6 Hz, 2 H), 2.60 (m, *J* = 5.3 Hz, 1 H). ESI-MS *m/z* (rel intensity) 292 (MH⁺, 100). HRMS (+ESI) calcd for MH⁺, 292.0974; found, 292.0978. HPLC purity: 96.6% (MeOH, 100%), 96.2% (MeOH–H₂O, 90:10).

6-(3-Hydroxypropyl)-5*H*-indeno[1,2-*c*]isoquinoline-5,11(6*H*)-dione (19).⁴² The general procedure provided the desired product as a red solid (1.20 g, 98%); mp 173–175 °C (lit.⁴² 170–171

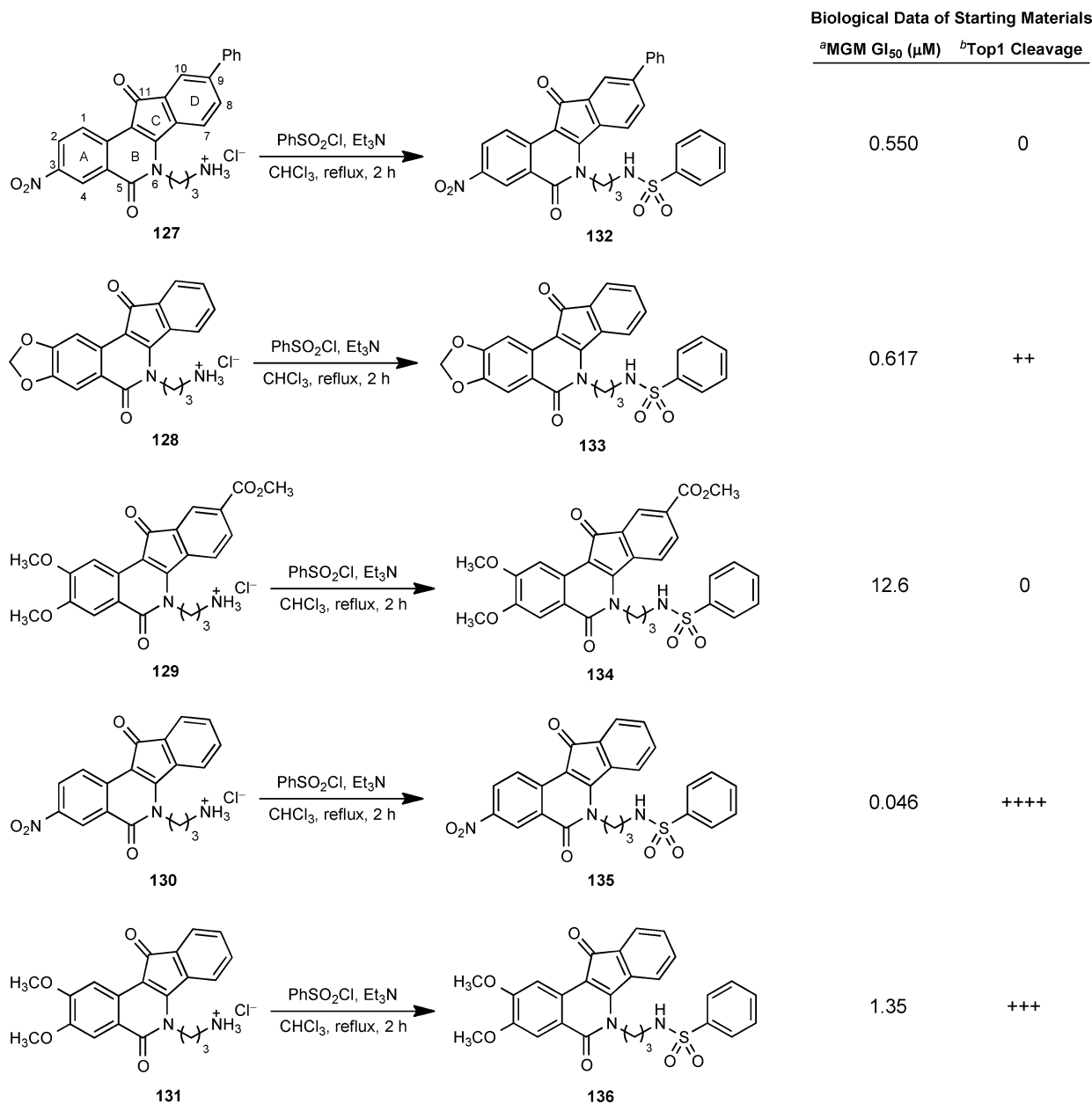


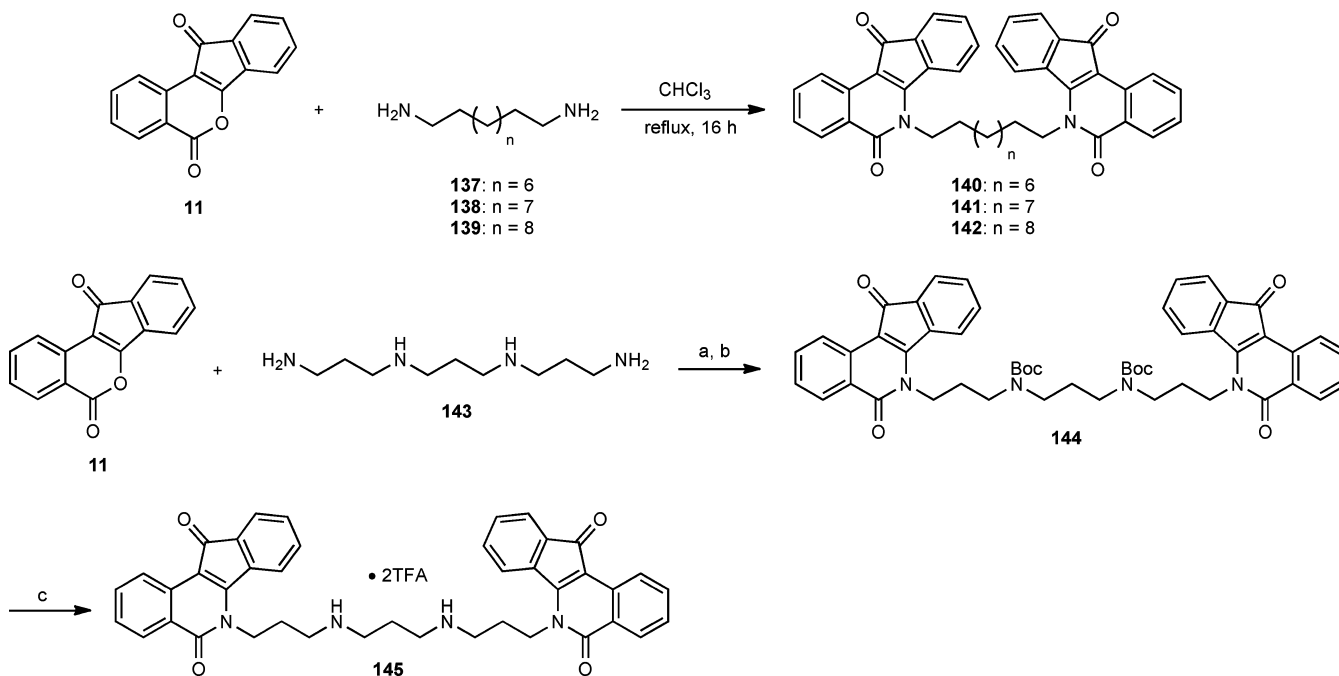
Figure 5. Ring-substituted indenoisoquinoline sulfonamides. ^aThe cytotoxicity GI₅₀ values are the concentrations corresponding to 50% growth inhibition. The MGM is the mean graph midpoint for growth inhibition of all 60 human cancer cell lines successfully tested, ranging from 10⁻⁸ to 10⁻⁴ molar, where values that fall outside the range were taken as 10⁻⁸ and 10⁻⁴ molar. ^bCompound-induced DNA cleavage due to Top1 inhibition is graded by the following semiquantitative relative to 1 μM camptothecin (1): 0, no inhibitory activity; +, between 20 and 50% activity; ++, between 50 and 75% activity; +++, between 75% and 95% activity; +++++, equipotent. The 0/+ ranking is between 0 and +.

°C). ¹H NMR (300 MHz, CDCl₃) δ 8.75 (d, *J* = 8.2 Hz, 1 H), 8.38 (d, *J* = 8.1 Hz, 1 H), 7.79–7.65 (m, 3 H), 7.53–7.41 (m, 3 H), 4.76 (t, *J* = 6.4 Hz, 2 H), 3.75 (q, *J* = 6.0 Hz, 2 H), 3.26 (t, *J* = 6.3 Hz, 1 H), 2.20 (m, 2 H). ESI-MS *m/z* (rel intensity) 328 (MNa⁺, 61). HRMS (+ESI) calcd for MH⁺, 306.1130; found, 306.1127. HPLC purity: 99.5% (MeOH, 100%), 98.6% (MeOH–H₂O, 90:10).

6-(4-Hydroxybutyl)-5H-indeno[1,2-c]isoquinoline-5,11(6H)-dione (20).⁴³ The general procedure provided the desired product as a red solid (1.23 g, 95%); mp 165–166 °C (lit.⁴³ 160–162 °C). ¹H NMR (300 MHz, CDCl₃) δ 8.73 (d, *J* = 8.1 Hz, 1 H), 8.36 (d, *J* = 8.3 Hz, 1 H), 7.76 (dt, *J* = 1.2 and 8.2 Hz, 1 H), 7.65 (dd, *J* = 1.4 and 6.7 Hz, 1 H), 7.59 (d, *J* = 7.6 Hz, 1 H), 7.50–7.38 (m, 3 H), 4.62 (t, *J* = 7.7 Hz, 2 H), 3.84 (q, *J* = 6.0 Hz, 2 H), 2.07 (m, 2 H), 1.86 (m, 2 H), 1.70 (t, *J* = 5.3 Hz, 1 H). ESI-MS *m/z* (rel intensity) 320 (MH⁺, 42). HRMS (+ESI) calcd for MH⁺, 320.1287; found, 320.1289. HPLC purity: 99.1% (MeOH, 100%), 96.2% (MeOH–H₂O, 90:10).

6-(5-Hydroxypentyl)-5H-indeno[1,2-c]isoquinoline-5,11(6H)-dione (21).⁴³ The general procedure provided the desired product as an orange solid (1.45 g, 90%); mp 144–146 °C (lit.⁴³ 146–148 °C). ¹H NMR (300 MHz, CDCl₃) δ 8.72 (d, *J* = 8.1 Hz, 1 H), 8.35 (d, *J* = 8.4 Hz, 1 H), 7.75 (dt, *J* = 1.2 and 7.0 Hz, 1 H), 7.65 (dd, *J* = 1.4 and 4.9 Hz, 1 H), 7.49–7.38 (m, 4 H), 4.56 (t, *J* = 7.7 Hz, 2 H), 3.74 (q, *J* = 5.3 Hz, 2 H), 1.98 (m, 2 H), 1.74–1.60 (m, 4 H), 1.42 (t, *J* = 4.8 Hz, 1 H). ESI-MS *m/z* (rel intensity) 334 (MH⁺, 100). HRMS (+ESI) calcd for MH⁺, 334.1443; found, 334.1445. HPLC purity: 97.9% (MeOH, 100%), 95.4% (MeOH–H₂O, 90:10).

6-(6-Hydroxyhexyl)-5H-indeno[1,2-c]isoquinoline-5,11(6H)-dione (22). The general procedure provided the desired product as a red solid (1.24 g, 84%); mp 139–141 °C. IR (film) 3425, 1765, 1698, 1663, 1611, 1550, 1504, 1427, 1317, 758 cm⁻¹. ¹H NMR (300 MHz, CDCl₃) δ 8.72 (d, *J* = 8.1 Hz, 1 H), 8.36 (d, *J* = 8.2 Hz, 1 H), 7.75 (dt, *J* = 1.3 and 7.4 Hz, 1 H), 7.65 (dd, *J* = 1.0 and 7.2 Hz, 1 H), 7.50–7.37

Scheme 9. Preparation of Bisindenoisoquinolines^a

^aReagents and conditions: (a) CHCl₃, reflux, 72 h; (b) Et₃N, Boc₂O, rt, 16 h; (c) TFA, rt.

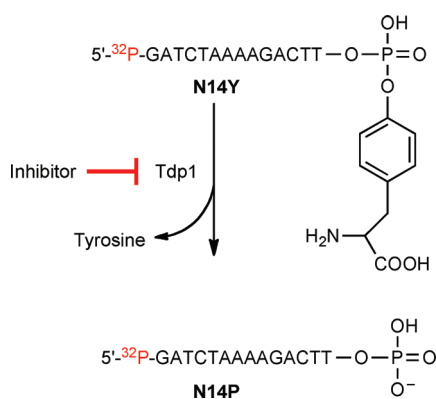


Figure 6. Schematic representation of the Tdp1 gel-based assays using recombinant Tdp1.

(m, 4 H), 4.56 (t, *J* = 7.7 Hz, 2 H), 3.70 (q, *J* = 5.7 Hz, 2 H), 3.50 (d, *J* = 4.9 Hz, 1 H), 1.96 (m, 2 H), 1.66–1.45 (m, 6 H). ESI-MS *m/z* (rel intensity) 370 (MNa⁺, 100). HRMS (+ESI) calcd for MNa⁺, 370.1419; found, 370.1424. HPLC purity: 97.6% (MeOH, 100%), 99.0% (MeOH–H₂O, 90:10).

6-(7-Hydroxyheptyl)-5H-indeno[1,2-*c*]isoquinoline-5,11(6H)-dione (23). Bromoalcohol 33 (0.975 g, 5.0 mmol) and urotropine (34, 0.771 g, 5.5 mmol) were dissolved in CHCl₃ (20 mL). The mixture was stirred at reflux for 5 h and allowed to stand overnight to induce the formation of quaternary salt 35. The salt was filtered and added to a 2 M ethanolic HCl solution (15 mL). The reaction mixture was warmed gently with a heat gun and swirled to produce white NH₄Cl precipitate, which was removed by filtration. The mother liquor was concentrated in vacuo and diluted in H₂O (20 mL), followed by cooling in an ice bath. The solution was made strongly alkaline (pH 13) with 6 M NaOH, extracted with diethyl ether (25 mL × 3), and washed with brine (25 mL). The ethereal layers were combined, dried over anhydrous Na₂SO₄, and concentrated to afford a yellowish oil of crude 17. The crude 17 was dissolved in CHCl₃ (20

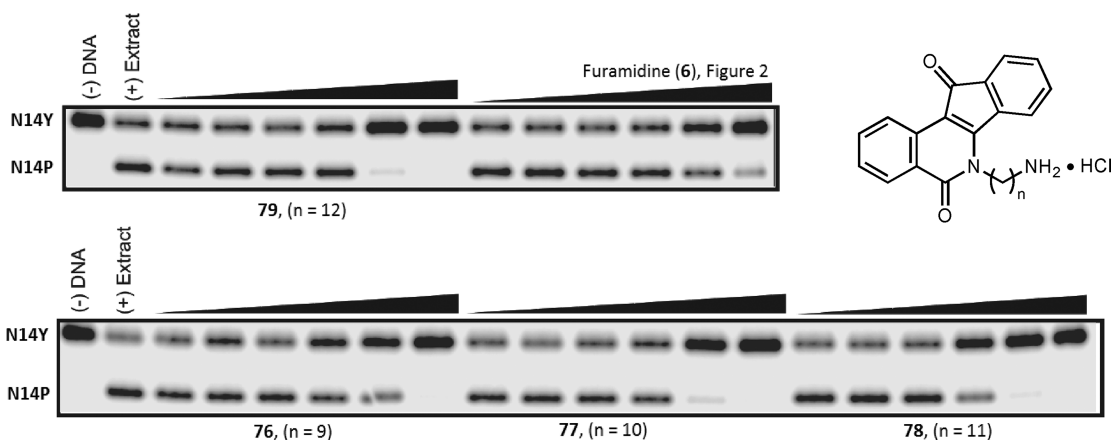
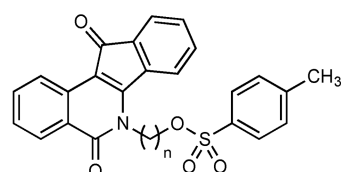
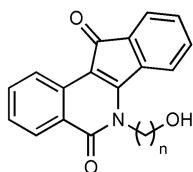
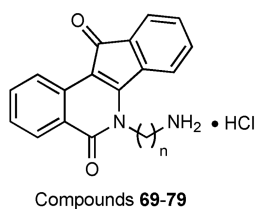


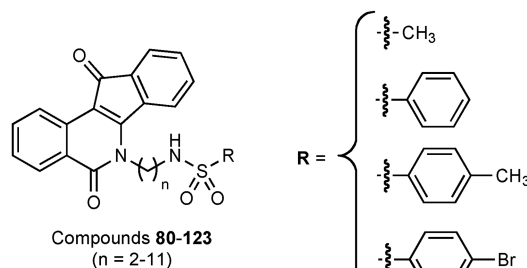
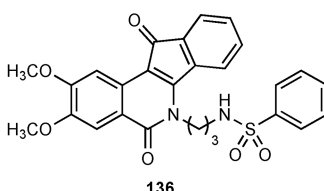
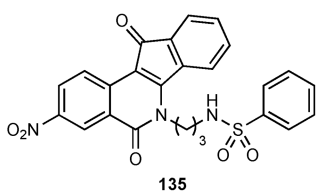
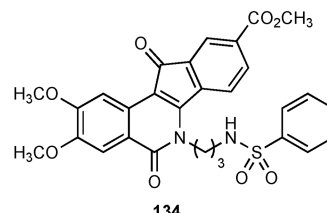
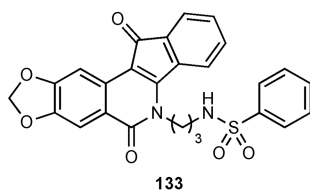
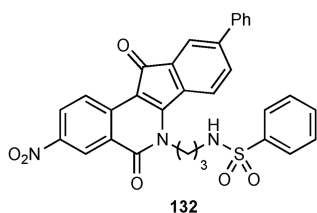
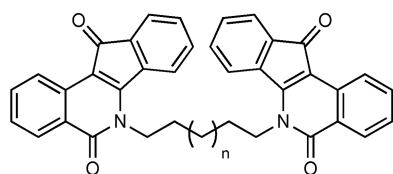
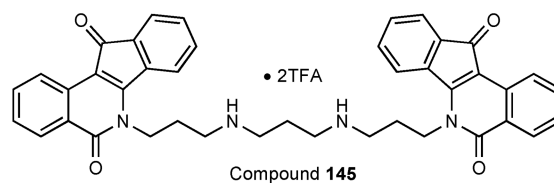
Figure 7. Representative gels showing concentration-dependent inhibition of endogenous Tdp1 in whole cell extract by indenoisoquinoline amine hydrochloride inhibitors. Concentrations were 0.5, 1.4, 4.1, 12.3, 37, and 111 μM.



Comp.	n	IC ₅₀ (μM) Tdp1		Top1
		rec.	WCE	
69	2	55.3±11.4	78	+++
70	3	29.5	29.5	+++
71	4	22.3	23.4	+++
72	5	17.5±4.5	28	0
73	6	25±5.5	35	++
74	7	28.8±6.8	31	0
75	8	48	49	+
76	9	47	48	0
77	10	14.1	21.3	0
78	11	12.8	14.1	+
79	12	15.1	33	0/+

Rec. = Recombinant Tdp1

WCE = Whole Cell Extract Tdp1

Compound **18-23**
(n = 2-7)All were inactive against Tdp1 (IC₅₀ > 111 μM).All were inactive against Tdp1 (IC₅₀ > 111 μM) and inactive against Top1 (0 or 0/+).All were inactive against Tdp1
(IC₅₀ > 111 μM).All were inactive against Tdp1
(IC₅₀ > 111 μM).

IC ₅₀ (μM) Tdp1		Top1
rec.	WCE	
1.52±0.05 (n=6)	1.9	++++

Figure 8. Inhibitory activities of target compounds against Tdp1 and Top1.

mL) and added to a solution of lactone **11** (1 equiv of **33**) in CHCl₃ (50 mL). The reaction mixture was heated at reflux for 18 h, concentrated, adsorbed onto SiO₂, and purified by flash column chromatography (SiO₂), eluting with EtOAc–hexane in a gradient of concentration ratios from 5:3 to 7:3 to provide the desired product as

a fine red powdery solid (0.95 g, 52%); mp 132–135 °C. IR (film) 3468, 1776, 1698, 1663, 1611, 1550, 1504, 1427, 1318, 756 cm⁻¹. ¹H NMR (300 MHz, CDCl₃) δ 8.72 (d, J = 8.0 Hz, 1 H), 8.36 (d, J = 8.1 Hz, 1 H), 7.72 (t, J = 7.0 Hz, 1 H), 7.65 (d, J = 6.4 Hz, 1 H), 7.49–7.40 (m, 4 H), 4.54 (t, J = 7.8 Hz, 2 H), 3.67 (d, J = 3.4 Hz, 2 H), 1.94–

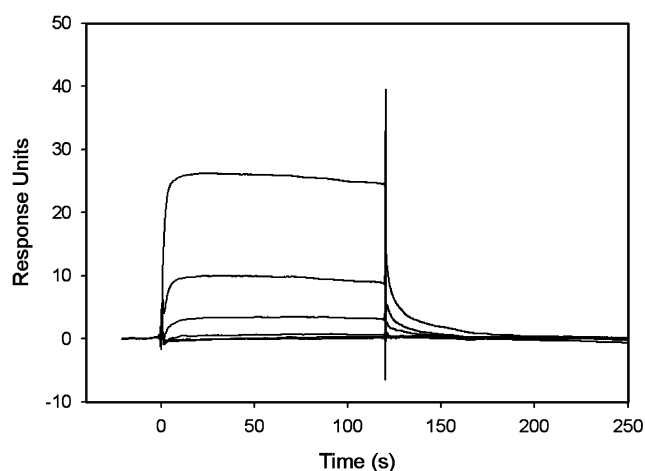


Figure 9. Direct binding of **70** to Tdp1 by surface plasmon resonance spectroscopy. Variable concentrations of **70** (33, 11, 3.7, 1.2, and 0.4 μM) were injected over amine coupled Tdp1 protein. The compound rapidly reaches equilibrium and then completely dissociates.

1.86 (m, 2 H), 1.62–1.43 (m, 8 H), 1.30 (m, 1 H). ESI-MS m/z (rel intensity) 362 (MH^+ , 17). HRMS (+ESI) calcd for MH^+ , 362.1756; found, 362.1760. Anal. Calcd for $\text{C}_{23}\text{H}_{23}\text{NO}_3 \cdot 0.2\text{H}_2\text{O}$: C, 75.68; H, 6.46; N, 3.84. Found: C, 75.51; H, 6.32; N, 3.62.

General Procedure for the Preparation of Indenoisoquinoline Sulfonates 25–29 and Chloride 30. A solution of Et_3N (2 equiv) in CH_2Cl_2 (1 mL) and DMAP (0.2 equiv) was added to solutions of the *n*-alkylhydroxy indenoisoquinolines **19–23** (100 mg) in CH_2Cl_2 (10 mL). The solutions were stirred at room temperature for 5 min, and tosyl chloride (2 equiv) was added. The reaction mixtures were stirred at room temperature for 16 h, quenched with aq 3 M HCl (50 mL), and washed with H_2O (50 mL), satd NaHCO_3 (50 mL), and brine (50 mL). The organic layers were dried over anhydrous Na_2SO_4 , filtered, and concentrated, purified by flash column chromatography (SiO_2), eluting with EtOAc (3–5%) in CHCl_3 , to provide the indenoisoquinoline sulfonates **25–29** in high purity after trituration with diethyl ether (20 mL).

3-(5,11-Dioxo-5H-indeno[1,2-c]isoquinolin-6(11H)-yl)propyl-4-methylbenzenesulfonate (25).⁴⁴ The general procedure provided the desired product as a red solid (132.5 mg, 88%); mp 177–179 $^\circ\text{C}$ (lit.⁴⁴ 180–182 $^\circ\text{C}$). ^1H NMR (300 MHz, CDCl_3) δ 8.72 (d, J = 8.1 Hz, 1 H), 8.31 (d, J = 7.5 Hz, 1 H), 7.83 (d, J = 8.3 Hz, 2 H), 7.73–7.63 (m, 3 H), 7.49–7.34 (m, 5 H), 4.62 (t, J = 7.9 Hz, 2 H), 4.31 (t, J = 5.7 Hz, 2 H), 2.46 (s, 3 H), 2.34 (m, 2 H). ESI-MS m/z (rel intensity) 482 (MNa^+ , 100). HRMS (+ESI) calcd for MNa^+ , 482.1038; found, 482.1041. HPLC purity: 98.6% (MeOH, 100%), 99.4% (MeOH– H_2O , 90:10).

4-(5,11-Dioxo-5H-indeno[1,2-c]isoquinolin-6(11H)-yl)butyl-4-methylbenzenesulfonate (26). The general procedure provided the desired product as an orange solid (129 mg, 87%); mp 160–163 $^\circ\text{C}$. IR (film) 1757, 1695, 1667, 1612, 1550, 1504, 1428, 1348, 1174, 753 cm^{-1} . ^1H NMR (300 MHz, CDCl_3) δ 8.72 (d, J = 8.0 Hz, 1 H), 8.32 (d, J = 7.4 Hz, 1 H), 7.78–7.70 (m, 3 H), 7.66 (d, J = 7.0 Hz, 1 H), 7.50–7.42 (m, 4 H), 7.33 (d, J = 8.2 Hz, 2 H), 4.55 (t, J = 6.8 Hz, 2 H), 4.16 (t, J = 5.9 Hz, 2 H), 2.42 (s, 3 H), 1.98–1.88 (m, 4 H). ESIMS m/z (rel intensity) 496 (MNa^+ , 100). HRMS (+ESI) calcd for MNa^+ , 496.1195; found, 496.1201. HPLC purity: 98.4% (MeOH, 100%), 99.2% (MeOH– H_2O , 90:10).

5-(5,11-Dioxo-5H-indeno[1,2-c]isoquinolin-6(11H)-yl)pentyl-4-methylbenzenesulfonate (27). The general procedure provided the desired product as an orange solid (119 mg, 81%); mp 163–165 $^\circ\text{C}$. IR (film) 1697, 1661, 1609, 1549, 1503, 1427, 1355, 1174, 755 cm^{-1} . ^1H NMR (300 MHz, CDCl_3) δ 8.73 (d, J = 8.1 Hz, 1 H), 8.34 (d, J = 7.8 Hz, 1 H), 7.79–7.70 (m, 3 H), 7.66 (d, J = 6.8 Hz, 1 H), 7.50–7.39 (m, 4 H), 7.34 (d, J = 8.1 Hz, 2 H), 4.51 (t, J = 7.8 Hz, 2 H), 4.09 (t, J = 6.1 Hz, 2 H), 2.43 (s, 3 H), 1.91–1.75 (m, 4 H), 1.65–1.57 (m, 2 H). ESI-MS m/z (rel intensity) 488 (MH^+ , 100). HRMS (+ESI) calcd for MH^+ , 488.1532; found, 488.1539. HPLC purity: 97.1% (MeOH, 100%), 98.0% (MeOH– H_2O , 90:10).

6-(5,11-Dioxo-5H-indeno[1,2-c]isoquinolin-6(11H)-yl)hexyl-4-methylbenzenesulfonate (28). The general procedure provided the desired product as an orange solid (123 mg, 85%); mp 146–149 $^\circ\text{C}$. IR (film) 1767, 1693, 1662, 1610, 1550, 1503, 1428, 1357, 1176, 757 cm^{-1} . ^1H NMR (300 MHz, CDCl_3) δ 8.72 (d, J = 8.2 Hz, 1 H), 8.34 (d, J = 7.9 Hz, 1 H), 7.80–7.70 (m, 3 H), 7.65 (d, J = 6.8 Hz, 1 H), 7.49–7.38 (m, 4 H), 7.36 (d, J = 8.0 Hz, 2 H), 4.51 (t, J = 7.6 Hz, 2 H), 4.07 (t, J = 6.3 Hz, 2 H), 2.44 (s, 3 H), 1.88 (m, 2 H), 1.73 (m, 2 H), 1.57 (m, 4 H). ESI-MS m/z (rel intensity) 502 (MH^+ , 100). HRMS (+ESI) calcd for MH^+ , 502.1688; found, 502.1694; HPLC purity: 98.0% (MeOH, 100%), 96.8% (MeOH– H_2O , 90:10).

7-(5,11-Dioxo-5H-indeno[1,2-c]isoquinolin-6(11H)-yl)heptyl-4-methylbenzenesulfonate (29). The general procedure provided the desired product as a red solid (109 mg, 76%); mp 123–126 $^\circ\text{C}$. IR (film) 1775, 1698, 1664, 1611, 1550, 1504, 1428, 1358, 1176, 758 cm^{-1} . ^1H NMR (300 MHz, CDCl_3) δ 8.72 (d, J = 8.0 Hz, 1 H), 8.35 (d, J = 7.6 Hz, 1 H), 7.80–7.70 (m, 3 H), 7.65 (d, J = 6.8 Hz, 1 H), 7.49–7.39 (m, 4 H), 7.35 (d, J = 8.1 Hz, 2 H), 4.51 (t, J = 7.7 Hz, 2 H), 4.05 (t, J = 6.3 Hz, 2 H), 2.44 (s, 3 H), 1.90 (m, 2 H), 1.67 (m, 2 H), 1.49 (m, 2 H), 1.40–1.37 (m, 4 H). ESI-MS m/z (rel intensity) 516 (MH^+ , 100). HRMS (+ESI) calcd for MH^+ , 516.1845; found, 516.1848. HPLC purity: 95.4% (MeOH, 100%), 98.3% (MeOH– H_2O , 90:10).

6-(2-Chloroethyl)-5H-indeno[1,2-c]isoquinoline-5,11(6H)-dione (30).⁴² The general procedure provided the chloride product as a purple solid (105 mg, 99%); mp 210–212 $^\circ\text{C}$ (lit.⁴² 197–199 $^\circ\text{C}$). ^1H NMR (300 MHz, CDCl_3) δ 8.73 (d, J = 8.0 Hz, 1 H), 8.36 (d, J = 8.2 Hz, 1 H), 7.78 (dt, J = 1.2 and 8.1 Hz, 1 H), 7.67 (d, J = 6.8 Hz, 1 H), 7.59 (d, J = 7.4 Hz, 1 H), 7.52–7.42 (m, 3 H), 4.86 (t, J = 7.4 Hz, 2 H), 3.97 (t, J = 7.7 Hz, 2 H). Probe EIMS m/z (rel intensity) 309

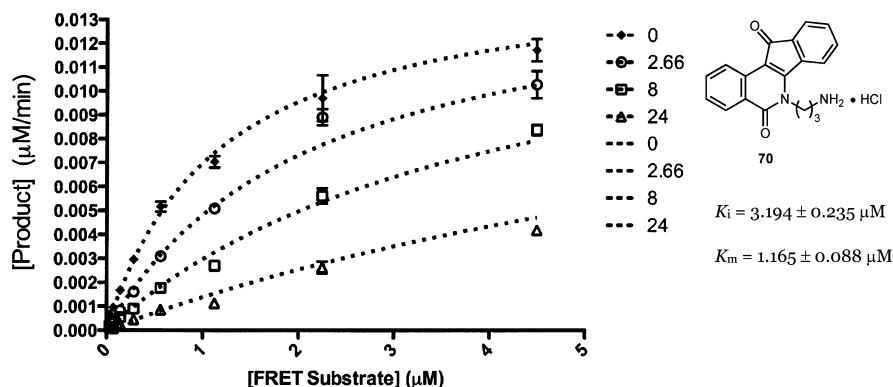


Figure 10. Competitive inhibition of **70** against recombinant Tdp1 measured by FRET assay.

(M⁺, 33). HRMS (EI) calcd for M⁺, 309.0557; found, 309.0560. HPLC purity: 95.3% (MeOH, 100%), 97.3% (MeOH–H₂O, 90:10).

2-(5,11-Dioxo-5H-indeno[1,2-c]isoquinolin-6(11H)-yl)ethyl Acetate (31). Et₃N (34.7 mg, 0.343 mmol), CH₃COOAg (57.2 mg, 0.343 mmol), and TsCl (65.4 mg, 0.343 mmol) were added to the solution of **18** (50 mg, 0.172 mmol) in CH₂Cl₂ (50 mL). The reaction mixture was stirred at room temperature for 16 h and then washed with satd NaHCO₃ (50 mL) and brine (50 mL). The organic layer was dried over Na₂SO₄, filtered, and concentrated, adsorbed onto SiO₂, and purified by flash column chromatography (SiO₂), eluting with EtOAc–CHCl₃ (2:8) to afford the desired product as a red solid (38.5 mg, 67%); mp 221–224 °C. IR (film) 1738, 1693, 1655, and 1506 cm⁻¹. ¹H NMR (300 MHz, CDCl₃) δ 8.75 (d, J = 8.0 Hz, 1 H), 8.37 (d, J = 7.9 Hz, 1 H), 7.75 (t, J = 5.8 Hz, 2 H), 7.67 (dd, J = 1.1 and 5.8 Hz, 1 H), 7.51–7.41 (m, 3 H), 4.84 (t, J = 6.2 Hz, 2 H), 4.57 (t, J = 6.1 Hz, 2 H), 1.94 (s, 3 H). Probe CIMS *m/z* (rel intensity) 334 (MH⁺, 100). HRMS (EI) calcd for M⁺, 333.1001; found, 333.1005. HPLC purity: 97.3% (MeOH, 100%), 98.0% (MeOH–H₂O, 90:10).

Compound **47–79** were synthesized based on the procedures reported by Morrell et al.³⁵ Purities of biologically tested indenoisoquinoline amine hydrochlorides **69–79** were ≥95% by HPLC (Table 2).

Table 2. Purities of Indenoisoquinoline Amine Hydrochlorides 69–79 by HPLC

compd	purity by HPLC	
	MeOH, 100%	MeOH–H ₂ O, 90:10
69	97.8	97.6
70	96.7	98.0
71	98.5	100
72	98.3	100
73	98.1	97.8
74	95.7	100
75	96.9	98.5
76	95.5	95.8
77	99.4	98.8
78	98.7	96.6
79	99.2	98.5

General Procedure for the Preparation of Indenoisoquinoline Sulfonamides 80–123. Indenoisoquinoline salts **69–79** (50 mg, 0.107–0.153 mmol) were dissolved in CHCl₃ (15 mL), followed by the addition of Et₃N (2 equiv) in CHCl₃ (1 mL). The solutions were stirred at room temperature for 5 min. Mesyl, benzenesulfonyl, tosyl, or *p*-bromobenzenesulfonyl chloride (2 equiv) were then added. The mixtures were heated at reflux for 16 h and then washed with satd NaHCO₃ (50 mL) and brine (50 mL). The organic layers were dried over anhydrous Na₂SO₄, filtered, and concentrated, and purified by flash column chromatography (SiO₂), eluting with EtOAc–CHCl₃ to provide the indenoisoquinoline sulfonamide products in high purity.

N-(2-(5,11-Dioxo-5H-indeno[1,2-c]isoquinolin-6(11H)ethyl)-methanesulfonamide (80). The crude product was eluted with EtOAc–CHCl₃ (4:6) to afford the desired product as an orange solid (38.7 mg, 69%); mp 250–255 °C. IR (film) 3313, 1705, 1653, 1609, 1549, 1502, 1418, 1321, 1129, 758 cm⁻¹. ¹H NMR (300 MHz, DMSO-*d*₆) δ 8.59 (d, J = 8.0 Hz, 1 H), 8.23 (d, J = 8.0 Hz, 1 H), 7.89–7.82 (m, 2 H), 7.58–7.47 (m, 5 H), 4.61 (t, J = 6.7 Hz, 2 H), 3.42 (m, 2 H), 2.91 (s, 3 H). Probe CIMS *m/z* (rel intensity) 369 (MH⁺, 100). HRMS (EI) calcd for M⁺, 368.0831; found, 368.0835. HPLC purity: 96.0% (MeOH, 100%), 96.3% (MeOH–H₂O, 90:10).

N-(3-(5,11-Dioxo-5H-indeno[1,2-c]isoquinolin-6(11H)-propyl)methanesulfonamide (81). The crude product was eluted with EtOAc–CHCl₃ (6:4) to afford the desired product as an orange solid (47.1 mg, 84%); mp 201–203 °C. IR (film) 3203, 1696, 1646, 1610, 1549, 1504, 1428, 1317, 1137, 757 cm⁻¹. ¹H NMR (300 MHz, CDCl₃) δ 8.72 (d, J = 8.1 Hz, 1 H), 8.32 (d, J = 8.1 Hz, 1 H), 7.77 (t, J = 7.0 Hz, 1 H), 7.65 (d, J = 6.5 Hz, 1 H), 7.55–7.38 (m, 4 H), 5.73 (t,

J = 6.8 Hz, 1 H), 4.70 (t, J = 6.0 Hz, 2 H), 3.25 (q, J = 6.5 Hz, 2 H), 3.00 (s, 3 H), 2.23–2.23 (m, 2 H). APCI-MS *m/z* (rel intensity) 383 (MH⁺, 100). HRMS (+ESI) calcd for MH⁺, 383.1066; found, 383.1069. HPLC purity: 99.1% (MeOH, 100%), 96.7% (MeOH–H₂O, 90:10).

N-(4-(5,11-Dioxo-5H-indeno[1,2-c]isoquinolin-6(11H)butyl)-methanesulfonamide (82). The crude product was eluted with EtOAc–CHCl₃ (7:3) to afford the desired product as an orange solid (42.2 mg, 81%); mp 193–194 °C. IR (film) 3272, 2346, 1694, 1655, 1611, 1549, 1504, 1318, 1152, 756 cm⁻¹. ¹H NMR (300 MHz, CDCl₃) δ 8.72 (d, J = 7.8 Hz, 1 H), 8.34 (d, J = 8.3 Hz, 1 H), 7.74 (t, J = 6.8 Hz, 1 H), 7.66 (d, J = 6.9 Hz, 1 H), 7.50–7.40 (m, 4 H), 4.60 (m, 3 H), 3.34 (q, J = 6.6 Hz, 2 H), 3.00 (s, 3 H), 2.05 (m, 2 H), 1.85 (m, 2 H). ESI-MS *m/z* (rel intensity) 397 (MH⁺, 100). HRMS (+ESI) calcd for MH⁺, 397.1222; found, 397.1231. HPLC purity: 98.4% (MeOH, 100%), 97.2% (MeOH–H₂O, 90:10).

N-(5-(5,11-Dioxo-5H-indeno[1,2-c]isoquinolin-6(11H)-pentyl)methanesulfonamide (83). The crude product was eluted with EtOAc–CHCl₃ (6:4) to afford the desired product as an orange solid (44.0 mg, 79%); mp 150–152 °C. IR (film) 3275, 1698, 1660, 1611, 1550, 1504, 1318, 1150, 756 cm⁻¹. ¹H NMR (300 MHz, CDCl₃) δ 8.72 (d, J = 8.0 Hz, 1 H), 8.34 (d, J = 8.0 Hz, 1 H), 7.76 (td, J = 7.1 and 1.1 Hz, 1 H), 7.65 (d, J = 6.9 Hz, 1 H), 7.50–7.41 (m, 4 H), 4.57 (t, J = 7.4 Hz, 2 H), 4.48 (t, J = 5.9 Hz, 1 H), 3.24 (q, J = 6.4 Hz, 2 H), 2.97 (s, 3 H), 2.00 (m, 2 H), 1.76 (m, 2 H), 1.65 (m, 2 H). ESI-MS *m/z* (rel intensity) 411 (MH⁺, 100). HRMS (+ESI) calcd for MH⁺, 411.1379; found, 411.1381. HPLC purity: 99.7% (MeOH, 100%), 98.5% (MeOH–H₂O, 90:10).

N-(6-(5,11-Dioxo-5H-indeno[1,2-c]isoquinolin-6(11H)hexyl)-methanesulfonamide (84). The crude product was eluted with EtOAc–CHCl₃ (5:5) to afford the desired product as an orange solid (42.7 mg, 77%); mp 160–161 °C. IR (film) 3355, 1697, 1646, 1608, 1548, 1504, 1452, 1364, 1258, 764 cm⁻¹. ¹H NMR (300 MHz, CDCl₃) δ 8.72 (d, J = 8.2 Hz, 1 H), 8.36 (d, J = 7.6 Hz, 1 H), 7.76 (dd, J = 7.0 and 1.2 Hz, 1 H), 7.65 (d, J = 6.8 Hz, 1 H), 7.50–7.41 (m, 4 H), 4.56 (t, J = 7.6 Hz, 1 H), 4.44 (m, 1 H), 3.20 (q, J = 6.5 Hz, 2 H), 2.97 (s, 3 H), 1.93 (m, 2 H), 1.67 (m, 2 H), 1.54 (m, 4 H). ESI-MS *m/z* (rel intensity) 425 (MH⁺, 100). HRMS (+ESI) calcd for MH⁺, 425.1538; found, 425.1532. HPLC purity: 99.8% (MeOH, 100%), 98.3% (MeOH–H₂O, 90:10).

N-(7-(5,11-Dioxo-5H-indeno[1,2-c]isoquinolin-6(11H)-heptyl)methanesulfonamide (85). The crude product was eluted with EtOAc–CHCl₃ (6:4) to afford the desired product as an orange solid (33 mg, 60%); mp 159–162 °C. IR (film) 3227, 1687, 1646, 1609, 1547, 1505, 1429, 1308, 1144, 754 cm⁻¹. ¹H NMR (300 MHz, CDCl₃) δ 8.72 (d, J = 8.1 Hz, 1 H), 8.36 (d, J = 8.2 Hz, 1 H), 7.73 (dd, J = 1.3 and 6.9 Hz, 1 H), 7.65 (d, J = 6.7 Hz, 1 H), 7.50–7.39 (m, 4 H), 4.54 (t, J = 7.8 Hz, 2 H), 4.24 (m, 1 H), 3.19 (q, J = 6.8 Hz, 2 H), 2.97 (s, 3 H), 1.91 (m, 2 H), 1.63–1.43 (m, 8 H). ESI-MS *m/z* (rel intensity) 461 (MNa⁺, 100). HRMS (+ESI) calcd for MNa⁺, 461.1511; found, 461.1518. Anal. Calcd for C₂₄H₂₆N₂O₄S·0.75H₂O: C, 63.77; H, 6.13; N, 6.20. Found: C, 63.73; H, 6.06; N, 5.86.

N-(8-(5,11-Dioxo-5H-indeno[1,2-c]isoquinolin-6(11H)octyl)-methanesulfonamide (86). The crude product was eluted with EtOAc–CHCl₃ (6:4) to afford the desired product as an orange solid (41.3 mg, 75%); mp 151–155 °C. IR (film) 3214, 1767, 1699, 1645, 1612, 1551, 1504, 1426, 1315, 1142, 760 cm⁻¹. ¹H NMR (300 MHz, CDCl₃) δ 8.73 (d, J = 8.0 Hz, 1 H), 8.36 (d, J = 8.0 Hz, 1 H), 7.75 (t, J = 7.1 Hz, 1 H), 7.66 (d, J = 6.8 Hz, 1 H), 7.50–7.39 (m, 4 H), 4.54 (t, J = 8.2 Hz, 2 H), 4.24 (m, 1 H), 3.17 (q, J = 6.9 Hz, 2 H), 2.96 (s, 3 H), 1.90 (m, 2 H), 1.57–1.26 (m, 10 H). ESI-MS *m/z* (rel intensity) 453 (MH⁺, 100). HRMS (+ESI) calcd for MH⁺, 453.1848; found, 453.1853. Anal. Calcd for C₂₅H₂₈N₂O₄S: C, 66.35; H, 6.24; N, 6.19. Found: C, 66.34; H, 6.31; N, 5.81.

N-(9-(5,11-Dioxo-5H-indeno[1,2-c]isoquinolin-6(11H)-nonyl)methanesulfonamide (87). The crude product was eluted with EtOAc–CHCl₃ (5:5) to afford the desired product as an orange solid (54.2 mg, 82%); mp 154–156 °C. IR (film) 3211, 1700, 1645, 1550, 1506, 1426, 1314, 1142, 759 cm⁻¹. ¹H NMR (300 MHz, CDCl₃) δ 8.73 (d, J = 8.1 Hz, 1 H), 8.36 (d, J = 7.7 Hz, 1 H), 7.73 (t, J = 8.2

Hz, 1 H), 7.66 (d, $J = 6.2$ Hz, 1 H), 7.50–7.40 (m, 4 H), 4.54 (t, $J = 8.0$ Hz, 2 H), 4.21 (m, 1 H), 3.17 (q, $J = 6.9$ Hz, 2 H), 2.96 (s, 3 H), 1.90 (m, 2 H), 1.63–1.23 (m, 12 H). ESI-MS m/z (rel intensity) 467 (MH⁺, 50). HRMS (+ESI) calcd for MH⁺, 467.2005; found, 467.2007. Anal. Calcd for C₂₆H₃₀N₂O₄S·0.2H₂O: C, 66.41; H, 6.52; N, 5.96. Found: C, 66.18; H, 6.39; N, 5.70.

N-(10-(5,11-Dioxo-5H-indeno[1,2-c]isoquinolin-6(11H)-decyl)methanesulfonamide (88). The crude product was eluted with EtOAc–CHCl₃ (3:7) to afford the desired product as an orange solid (45.3 mg, 83%); mp 115–117 °C. IR (film) 3297, 1697, 1663, 1611, 1551, 1505, 1428, 1351, 1175, 759 cm⁻¹. ¹H NMR (300 MHz, CDCl₃) δ 8.72 (d, $J = 8.1$ Hz, 1 H), 8.35 (d, $J = 7.5$ Hz, 1 H), 7.72 (t, $J = 6.9$ Hz, 1 H), 7.65 (d, $J = 6.3$ Hz, 1 H), 7.49–7.40 (m, 4 H), 4.53 (t, $J = 7.9$ Hz, 2 H), 4.20 (br s, 1 H), 3.16 (q, $J = 6.8$ Hz, 2 H), 2.95 (s, 3 H), 1.93 (m, 2 H), 1.56–1.18 (m, 14 H). ESI-MS m/z (rel intensity) 481 (MH⁺, 100). HRMS (+ESI) calcd for MH⁺, 481.2161; found, 481.2165. HPLC purity: 95.7% (MeOH, 100%), 96.2% (MeOH–H₂O, 90:10).

N-(11-(5,11-Dioxo-5H-indeno[1,2-c]isoquinolin-6(11H)-yl)-undecyl)methanesulfonamide (89). The crude product was eluted with EtOAc–CHCl₃ (5:5) to afford the desired product as an orange solid (48.7 mg, 89%); mp 136–137 °C. IR (film) 3299, 1699, 1658, 1612, 1577, 1504, 1424, 1312, 1134, 761 cm⁻¹. ¹H NMR (300 MHz, CDCl₃) δ 8.72 (d, $J = 8.2$ Hz, 1 H), 8.35 (d, $J = 8.1$ Hz, 1 H), 7.75 (t, $J = 7.3$ Hz, 1 H), 7.65 (d, $J = 6.3$ Hz, 1 H), 7.49–7.40 (m, 4 H), 4.53 (t, $J = 7.8$ Hz, 2 H), 4.25 (br s, 1 H), 3.16 (q, $J = 6.6$ Hz, 2 H), 2.96 (s, 3 H), 1.90 (m, 2 H), 1.61–1.25 (m, 16 H). ESI-MS m/z (rel intensity) 495 (MH⁺, 100). HRMS (+ESI) calcd for MH⁺, 495.2318; found, 495.2322. HPLC purity: 97.4% (MeOH, 100%), 100% (MeOH–H₂O, 90:10).

N-(12-(5,11-Dioxo-5H-indeno[1,2-c]isoquinolin-6(11H)-yl)-dodecyl)methanesulfonamide (90). The crude product was eluted with EtOAc–CHCl₃ (5:5) to afford the desired product as an orange solid (58.0 mg, 89%); mp 113–117 °C. IR (film) 3268, 1698, 1662, 1610, 1550, 1504, 1427, 1318, 1151, 759 cm⁻¹. ¹H NMR (300 MHz, CDCl₃) δ 8.71 (d, $J = 8.0$ Hz, 1 H), 8.35 (d, $J = 8.0$ Hz, 1 H), 7.74 (t, $J = 7.7$ Hz, 1 H), 7.64 (d, $J = 6.5$ Hz, 1 H), 7.49–7.40 (m, 4 H), 4.52 (t, $J = 7.7$ Hz, 2 H), 4.26 (m, 1 H), 3.16 (dd, $J = 13$ and 6.7 Hz, 2 H), 2.95 (s, 3 H), 1.89 (m, 14 H). APCI-MS m/z (rel intensity) 509 (MH⁺, 100). HRMS (+ESI) calcd for MNa⁺, 531.2294; found, 531.2291. HPLC purity: 99.2% (CH₃CN, 100%), 98.3% (CH₃CN–H₂O, 90:10).

N-(2-(5,11-Dioxo-5H-indeno[1,2-c]isoquinolin-6(11H)ethyl)-benzenesulfonamide (91). The crude product was eluted with EtOAc–CHCl₃ (2:8) to afford the desired product as an orange solid (47.8 mg, 72%); mp 246–249 °C. IR (film) 3233, 1702, 1652, 1610, 1551, 1505, 1425, 1342, 1157, 756 cm⁻¹. ¹H NMR (300 MHz, DMSO-*d*₆) δ 8.54 (d, $J = 8.1$ Hz, 1 H), 8.18–8.13 (m, 2 H), 7.80–7.72 (m, 4 H), 7.58–7.48 (m, 7 H), 4.55 (t, $J = 6.9$ Hz, 2 H), 3.23 (t, $J = 6.8$ Hz, 2 H). ESI-MS m/z (rel intensity) 431 (MH⁺, 13). HRMS (+ESI) calcd for MH⁺, 431.1066; found, 431.1073. HPLC purity: 95.9% (MeOH, 100%), 98.0% (MeOH–H₂O, 90:10).

N-(3-(5,11-Dioxo-5H-indeno[1,2-c]isoquinolin-6(11H)-yl)-propyl)benzenesulfonamide (92). The crude product was eluted with EtOAc–CHCl₃ (2:8) to afford the desired product as a red solid (57.2 mg, 88%); mp 216–218 °C. IR (film) 3282, 1655, 1611, 1550, 1502, 1446, 1317, 1161, 748 cm⁻¹. ¹H NMR (300 MHz, CDCl₃) δ 8.72 (d, $J = 8.0$ Hz, 1 H), 8.31 (d, $J = 8.1$ Hz, 1 H), 7.90–7.88 (m, 2 H), 7.78 (d, $J = 8.3$ Hz, 1 H), 7.65 (d, $J = 5.9$ Hz, 1 H), 7.51–7.38 (m, 7 H), 5.96 (t, $J = 5.0$ Hz, 1 H), 4.67 (t, $J = 6.2$ Hz, 2 H), 3.01 (q, $J = 4.8$ Hz, 2 H), 2.15 (m, 2 H). APCI-MS m/z (rel intensity) 445 (MH⁺, 100). HRMS (+ESI) calcd for MNa⁺, 467.1042; found, 467.1047. HPLC purity: 95.8% (MeOH, 100%), 95.1% (MeOH–H₂O, 95:5).

N-(4-(5,11-Dioxo-5H-indeno[1,2-c]isoquinolin-6(11H)-yl)-butyl)benzenesulfonamide (93). The crude product was eluted with EtOAc–CHCl₃ (3:7) to afford the desired product as a red solid (57.2 mg, 89%); mp 184–186 °C. IR (film) 3222, 1700, 1652, 1614, 1551, 1507, 1427, 1324, 1164, 753 cm⁻¹. ¹H NMR (300 MHz, CDCl₃) δ 8.71 (d, $J = 8.0$ Hz, 1 H), 8.32 (d, $J = 8.0$ Hz, 1 H), 7.89 (d, $J = 6.9$ Hz, 2 H), 7.75 (t, $J = 7.1$ Hz, 1 H), 7.65 (d, $J = 7.1$ Hz, 1 H), 7.56–

7.39 (m, 7 H), 4.83 (t, $J = 6.2$ Hz, 1 H), 4.54 (t, $J = 7.5$ Hz, 2 H), 3.14 (q, $J = 6.5$ Hz, 2 H), 1.98 (m, 2 H), 1.78 (m, 2 H). ESI-MS m/z (rel intensity) 459 (MH⁺, 100). HRMS (+ESI) calcd for MH⁺, 459.1379; found, 459.1375. HPLC purity: 98.5% (MeOH, 100%), 98.3% (MeOH–H₂O, 90:10).

N-(5-(5,11-Dioxo-5H-indeno[1,2-c]isoquinolin-6(11H)-yl)-pentyl)benzenesulfonamide (94). The crude product was eluted with EtOAc–CHCl₃ (2:8) to afford the desired product as an orange solid (55.8 mg, 84%); mp 194–195 °C. IR (film) 3284, 1728, 1699, 1662, 1609, 1548, 1504, 1446, 1326, 1261, 1161, 758 cm⁻¹. ¹H NMR (300 MHz, CDCl₃) δ 8.72 (d, $J = 8.1$ Hz, 1 H), 8.36 (d, $J = 8.4$ Hz, 1 H), 7.87 (dd, $J = 1.5$ and 5.4 Hz, 2 H), 7.76 (td, $J = 1.3$ and 7.0 Hz, 1 H), 7.65 (d, $J = 6.8$ Hz, 1 H), 7.57–7.38 (m, 7 H), 4.66 (t, $J = 6.1$ Hz, 1 H), 4.52 (t, $J = 7.5$ Hz, 2 H), 3.05 (q, $J = 6.3$ Hz, 2 H), 1.91 (m, 2 H), 1.67 (m, 2 H), 1.58 (m, 2 H). ESI-MS m/z (rel intensity) 473 (MH⁺, 100). HRMS (+ESI) calcd for MH⁺, 473.1535; found, 473.1532. HPLC purity: 99.5% (MeOH, 100%), 98.7% (MeOH–H₂O, 90:10).

N-(6-(5,11-Dioxo-5H-indeno[1,2-c]isoquinolin-6(11H)-yl)-hexyl)benzenesulfonamide (95). The crude product was eluted with EtOAc–CHCl₃ (2:8) to afford the desired product as an orange solid (57.8 mg, 91%); mp 150–152 °C. IR (film) 3272, 1698, 1663, 1503, 1427, 1320, 1159, 756 cm⁻¹. ¹H NMR (300 MHz, CDCl₃) δ 8.73 (d, $J = 8.1$ Hz, 1 H), 8.35 (d, $J = 7.6$ Hz, 1 H), 7.89 (dd, $J = 6.7$ and 1.6 Hz, 2 H), 7.76 (t, $J = 8.2$ Hz, 1 H), 7.66 (d, $J = 6.9$ Hz, 1 H), 7.58–7.41 (m, 7 H), 4.56–4.48 (m, 3 H), 3.03 (q, $J = 6.3$ Hz, 2 H), 1.88 (m, 2 H), 1.56–1.48 (m, 6 H). ESI-MS m/z (rel intensity) 509 (MNa⁺, 100). HRMS (+ESI) calcd for MNa⁺, 509.1511; found, 509.1521. HPLC purity: 97.9% (MeOH, 100%), 97.4% (MeOH–H₂O, 90:10).

N-(7-(5,11-Dioxo-5H-indeno[1,2-c]isoquinolin-6(11H)-yl)-heptyl)benzenesulfonamide (96). The crude product was eluted with EtOAc–CHCl₃ (2:8) to afford the desired compound as an orange product (37.8 mg, 75%); mp 178–181 °C. IR (film) 3281, 1698, 1669, 1608, 1548, 1504, 1446, 1324, 1160, 759 cm⁻¹. ¹H NMR (300 MHz, CDCl₃) δ 8.73 (d, $J = 8.1$ Hz, 1 H), 8.37 (d, $J = 8.0$ Hz, 1 H), 7.88 (dd, $J = 0.92$ and 6.8 Hz, 2 H), 7.66 (t, $J = 6.7$ Hz, 1 H), 7.57 (d, $J = 6.9$ Hz, 1 H), 7.54–7.43 (m, 7 H), 4.52 (t, $J = 6.8$ Hz, 3 H), 3.01 (q, $J = 6.6$ Hz, 2 H), 1.87 (m, 2 H), 1.49–1.25 (m, 8 H). ESI-MS m/z (rel intensity) 501 (MH⁺, 45). HRMS (+ESI) calcd for MNa⁺, 523.1668; found, 523.1672. Anal. Calcd for C₂₉H₂₈N₂O₄S·0.7H₂O: C, 67.87; H, 5.77; N, 5.46. Found: C, 67.50; H, 5.40; N, 5.37.

N-(8-(5,11-Dioxo-5H-indeno[1,2-c]isoquinolin-6(11H)-yl)-octyl)benzenesulfonamide (97). The crude product was eluted with EtOAc–CHCl₃ (2:8) to afford the desired compound as an orange product (36.1 mg, 72%); mp 136–140 °C. IR (film) 3271, 1698, 1663, 1504, 1427, 1320, 1159, 756 cm⁻¹. ¹H NMR (300 MHz, CDCl₃) δ 8.73 (d, $J = 8.1$ Hz, 1 H), 8.36 (d, $J = 8.0$ Hz, 1 H), 7.88 (d, $J = 6.9$ Hz, 2 H), 7.70 (t, $J = 7.0$ Hz, 1 H), 7.66 (d, $J = 6.7$ Hz, 1 H), 7.61–7.38 (m, 7 H), 4.52 (t, $J = 7.8$ Hz, 2 H), 4.36 (m, 1 H), 3.00 (q, $J = 6.8$ Hz, 2 H), 1.91 (m, 2 H), 1.47–1.25 (m, 10 H). ESI-MS m/z (rel intensity) 1051 (M₂Na⁺, 100). HRMS (+ESI) calcd for MH⁺, 515.2005; found, 515.2014; HPLC purity: 99.4% (MeOH, 100%), 99.3% (MeOH–H₂O, 90:10).

N-(9-(5,11-Dioxo-5H-indeno[1,2-c]isoquinolin-6(11H)-yl)-nonyl)benzenesulfonamide (98). The crude product was eluted with EtOAc–CHCl₃ (6:4) to afford the desired compound as an orange solid (58.2 mg, 78%); mp 162–164 °C. ¹H NMR (300 MHz, CDCl₃) δ 8.73 (d, $J = 7.9$ Hz, 1 H), 8.36 (d, $J = 8.4$ Hz, 1 H), 7.87 (d, $J = 7.0$ Hz, 2 H), 7.84–7.43 (m, 9 H), 4.53 (t, $J = 8.1$ Hz, 2 H), 4.38 (m, 1 H), 2.99 (q, $J = 6.9$ Hz, 2 H), 1.89 (m, 2 H), 1.57–1.25 (m, 12 H). ESI-MS m/z (rel intensity) 551 (MNa⁺, 100). HRMS (+ESI) calcd for MH⁺, 529.2161; found, 529.2159. HPLC purity: 100% (MeOH, 100%), 96.0% (MeOH–H₂O, 90:10).

N-(10-(5,11-Dioxo-5H-indeno[1,2-c]isoquinolin-6(11H)-yl)-decyl)benzenesulfonamide (99). The crude product was eluted with EtOAc–CHCl₃ (15:85) to afford the desired product as an orange solid (54.6 mg, 88%); mp 128–130 °C. IR (film) 3274, 1698, 1667, 1611, 1550, 1505, 1428, 1320, 1160, 757 cm⁻¹. ¹H NMR (300 MHz, CDCl₃) δ 8.72 (d, $J = 8.1$ Hz, 1 H), 8.36 (d, $J = 8.2$ Hz, 1 H),

7.88 (dd, $J = 1.5$ and 5.3 Hz, 2 H), 7.73 (dt, $J = 1.3$ and 7.0 Hz, 1 H), 7.66 (d, $J = 6.2$ Hz, 1 H), 7.57–7.40 (m, 7 H), 4.53 (t, $J = 7.6$ Hz, 2 H), 4.37 (t, $J = 6.1$ Hz, 1 H), 2.99 (q, $J = 6.7$ Hz, 2 H), 1.90 (m, 2 H), 1.52–1.24 (m, 14 H). APCI-MS m/z (rel intensity) 543 (MH^+ , 100). HRMS (+APCI) calcd for MNa^+ , 565.2137; found, 565.2142. HPLC purity: 100% (MeOH, 100%), 99.4% (MeOH–H₂O, 90:10).

***N*-(11-(5,11-Dioxo-5*H*-indeno[1,2-*c*]isoquinolin-6(11*H*)-yl)-undecyl)benzenesulfonamide (100).** The crude product was eluted with EtOAc–CHCl₃ (6:4) to afford the desired compound as a red solid (53.4 mg, 87%); mp 170–172 °C. IR (film) 3289, 1698, 1669, 1609, 1548, 1445, 1326, 1160, 760 cm⁻¹. ¹H NMR (300 MHz, CDCl₃) δ 8.73 (d, $J = 8.0$ Hz, 1 H), 8.36 (d, $J = 8.4$ Hz, 1 H), 7.88 (dd, $J = 1.6$ and 6.9 Hz, 2 H), 7.76 (dt, $J = 1.2$ and 7.1 Hz, 1 H), 7.66 (d, $J = 6.2$ Hz, 1 H), 7.61–7.39 (m, 7 H), 4.53 (t, $J = 8.1$ Hz, 2 H), 4.38 (m, 1 H), 2.99 (q, $J = 6.9$ Hz, 2 H), 1.89 (m, 2 H), 1.57–1.25 (m, 16 H). ESI-MS m/z (rel intensity) 557 (MH^+ , 100). HRMS (+ESI) calcd for MH^+ , 557.2474; found, 557.2477. HPLC purity: 98.8% (MeOH, 100%), 100% (MeOH–H₂O, 90:10).

***N*-(12-(5,11-Dioxo-5*H*-indeno[1,2-*c*]isoquinolin-6(11*H*)-yl)-dodecyl)benzenesulfonamide (101).** The crude product was eluted with EtOAc–CHCl₃ (7:3) to afford the desired compound as an orange solid (62.8 mg, 86%); mp 128–130 °C. IR (film) 3275, 1698, 1662, 1610, 1504, 1426, 1319, 1159, 756 cm⁻¹. ¹H NMR (300 MHz, CDCl₃) δ 8.72 (d, $J = 8.1$ Hz, 1 H), 8.35 (d, $J = 8.1$ Hz, 1 H), 7.87 (d, $J = 7.0$ Hz, 2 H), 7.84–7.42 (m, 9 H), 4.52 (t, $J = 7.6$ Hz, 2 H), 4.39 (m, 1 H), 2.98 (q, $J = 6.7$ Hz, 2 H), 1.89 (m, 2 H), 1.59–1.21 (m, 12 H). ESI-MS m/z (rel intensity) 571 (MH^+ , 100). HRMS (+ESI) calcd for MH^+ , 571.2631; found, 571.2628. Anal. Calcd for C₃₄H₃₈N₂O₄S: C, 71.55; H, 6.71; N, 4.91. Found: C, 71.70; H, 6.82; N, 5.09.

***N*-(2-(5,11-Dioxo-5*H*-indeno[1,2-*c*]isoquinolin-6(11*H*)-ethyl)-4-methylbenzenesulfonamide (102).** The crude product was eluted with EtOAc–CHCl₃ (2:8) to afford the desired product as an orange solid (57.4 mg, 84%); mp 272–274 °C. IR (film) 3209, 1702, 1646, 1611, 1552, 1506, 1427, 1322, 1147, 763 cm⁻¹. ¹H NMR (300 MHz, DMSO-*d*₆) δ 8.55 (d, $J = 8.0$ Hz, 1 H), 8.18 (d, $J = 7.6$ Hz, 1 H), 8.01 (m, 1 H), 7.83–7.76 (m, 2 H), 7.58–7.48 (m, 6 H), 7.26 (d, $J = 8.1$ Hz, 2 H), 4.53 (t, $J = 7.0$ Hz, 2 H), 3.24 (t, $J = 6.7$ Hz, 2 H), 2.29 (s, 3 H). ESI-MS m/z (rel intensity) 443 ($[M - H]^-$, 100). HRMS (+ESI) calcd for MH^+ , 445.1222; found, 445.1220. HPLC purity: 98.6% (MeOH, 100%), 96.4% (MeOH–H₂O, 90:10).

***N*-(3-(5,11-Dioxo-5*H*-indeno[1,2-*c*]isoquinolin-6(11*H*)-yl)-propyl)-4-methylbenzenesulfonamide (103).** The crude product was eluted with EtOAc–CHCl₃ (3:7) to afford the desired product as an orange solid (58.8 mg, 87%); mp 213–216 °C. IR (film) 3294, 1705, 1638, 1609, 1548, 1501, 1422, 1327, 1163, 758 cm⁻¹. ¹H NMR (300 MHz, DMSO-*d*₆) δ 8.58 (d, $J = 8.1$ Hz, 1 H), 8.21 (d, $J = 8.4$ Hz, 1 H), 7.82–7.74 (m, 3 H), 7.65–7.63 (m, 2 H), 7.59–7.50 (m, 4 H), 7.33–7.31 (m, 2 H), 4.49 (t, $J = 7.5$ Hz, 2 H), 2.93 (m, 2 H), 2.33 (s, 3 H), 1.92 (m, 2 H). ESI-MS m/z (rel intensity) 459 (MH^+ , 100). HRMS (+ESI) calcd for MH^+ , 459.1379; found, 459.1384. HPLC purity: 100% (MeOH, 100%), 99.4% (MeOH–H₂O, 90:10).

***N*-(4-(5,11-Dioxo-5*H*-indeno[1,2-*c*]isoquinolin-6(11*H*)-butyl)-4-methylbenzenesulfonamide (104).** The crude product was eluted with EtOAc–CHCl₃ (2:8) to afford the desired product as an orange solid (59.7 mg, 90%); mp 190–192 °C. IR (film) 3272, 1699, 1661, 1606, 1545, 1501, 1424, 1312, 1154, 759 cm⁻¹. ¹H NMR (300 MHz, CDCl₃) δ 8.71 (d, $J = 8.1$ Hz, 1 H), 8.32 (d, $J = 7.5$ Hz, 1 H), 7.76–7.70 (m, 3 H), 7.64 (d, $J = 6.9$ Hz, 1 H), 7.50–7.41 (m, 4 H), 7.30–7.26 (m, 2 H), 4.76 (t, $J = 6.3$ Hz, 1 H), 4.54 (t, $J = 7.5$ Hz, 2 H), 3.11 (q, $J = 6.5$ Hz, 2 H), 2.40 (s, 3 H), 1.98 (m, 2 H), 1.76 (m, 2 H). ESI-MS m/z (rel intensity) 473 (MH^+ , 100). HRMS (+ESI) calcd for MNa^+ , 495.1355; found, 495.1362. HPLC purity: 96.4% (CH₃CN, 100%), 97.1% (CH₃CN–H₂O, 90:10).

***N*-(5-(5,11-Dioxo-5*H*-indeno[1,2-*c*]isoquinolin-6(11*H*)-pentyl)-4-methylbenzenesulfonamide (105).** The crude product was eluted with EtOAc–CHCl₃ (15:85) to afford the desired product as an orange solid (61.5 mg, 93%); mp 187–188 °C. IR (film) 3273, 1694, 1671, 1609, 1548, 1504, 1426, 1325, 1159, 758 cm⁻¹. ¹H NMR (300 MHz, CDCl₃) δ 8.72 (d, $J = 8.1$ Hz, 1 H), 8.35 (d, $J = 7.4$ Hz, 1

H), 7.76–7.70 (m, 3 H), 7.65 (d, $J = 6.8$ Hz, 1 H), 7.50–7.38 (m, 4 H), 7.30–7.27 (m, 2 H), 4.55 (m, 3 H), 3.02 (q, $J = 6.4$ Hz, 2 H), 2.41 (s, 3 H), 1.90 (m, 2 H), 1.65 (m, 2 H), 1.54 (m, 2 H). ESI-MS m/z (rel intensity) 487 (MH^+ , 100). HRMS (+ESI) calcd for MH^+ , 487.1692; found, 487.1688. HPLC purity: 99.2% (MeOH, 100%), 98.1% (MeOH–H₂O, 90:10).

***N*-(6-(5,11-Dioxo-5*H*-indeno[1,2-*c*]isoquinolin-6(11*H*)-hexyl)-4-methylbenzenesulfonamide (106).** The crude product was eluted with EtOAc–CHCl₃ (2:8) to afford the desired product as a red solid (60.2 mg, 92%); mp 146–149 °C. IR (film) 3583, 1688, 1652, 1608, 1500, 1419, 1314, 1151, 759 cm⁻¹. ¹H NMR (300 MHz, CDCl₃) δ 8.73 (d, $J = 8.0$ Hz, 1 H), 8.35 (d, $J = 8.1$ Hz, 1 H), 7.76–7.71 (m, 3 H), 7.66 (d, $J = 6.7$ Hz, 1 H), 7.50–7.40 (m, 4 H), 7.30–7.27 (m, 2 H), 4.53 (m, 3 H), 3.00 (q, $J = 6.2$ Hz, 2 H), 2.42 (s, 3 H), 1.88 (m, 2 H), 1.53–1.48 (m, 6 H). ESI-MS m/z (rel intensity) 501 (MH^+ , 100). HRMS (+ESI) calcd for MH^+ , 501.1848; found, 501.1860. HPLC purity: 96.4% (MeOH, 100%), 97.6% (MeOH–H₂O, 90:10).

***N*-(7-(5,11-Dioxo-5*H*-indeno[1,2-*c*]isoquinolin-6(11*H*)-yl)-heptyl)-4-methylbenzenesulfonamide (107).** The crude product was eluted with EtOAc–CHCl₃ (6:4) to afford the desired compound as an orange solid (41.5 mg, 80%); mp 173–175 °C. IR (film) 3275, 1696, 1663, 1609, 1575, 1549, 1503, 1426, 1321, 1158, 780 cm⁻¹. ¹H NMR (300 MHz, CDCl₃) δ 8.72 (d, $J = 7.7$ Hz, 1 H), 8.36 (d, $J = 8.4$ Hz, 1 H), 7.76–7.73 (m, 3 H), 7.65 (d, $J = 5.9$ Hz, 1 H), 7.50–7.45 (m, 4 H), 7.31–7.29 (m, 2 H), 4.49 (m, 3 H), 2.96 (q, $J = 6.5$ Hz, 2 H), 2.42 (s, 3 H), 1.87 (m, 2 H), 1.49–1.25 (m, 8 H). ESI-MS m/z (rel intensity) 537 (MNa^+ , 100). HRMS (+ESI) calcd for MNa^+ , 537.1824; found, 537.1819. Anal. Calcd for C₃₀H₃₀N₂O₄S·0.7H₂O: C, 68.34; H, 6.00; N, 5.31. Found: C, 67.97; H, 5.75; N, 4.96.

***N*-(8-(5,11-Dioxo-5*H*-indeno[1,2-*c*]isoquinolin-6(11*H*)-yl)-octyl)-4-methylbenzenesulfonamide (108).** The crude product was eluted with EtOAc–CHCl₃ (6:4) to afford the desired compound as an orange solid (36.0 mg, 70%); mp 136–139 °C. IR (film) 3272, 1698, 1663, 1611, 1550, 1504, 1428, 1320, 1159, 757 cm⁻¹. ¹H NMR (300 MHz, CDCl₃) δ 8.73 (d, $J = 8.0$ Hz, 1 H), 8.36 (d, $J = 8.1$ Hz, 1 H), 7.75–7.70 (m, 3 H), 7.66 (d, $J = 6.9$ Hz, 1 H), 7.50–7.40 (m, 4 H), 7.32 (d, $J = 8.0$ Hz, 2 H), 4.53 (t, $J = 8.2$ Hz, 2 H), 4.31 (m, 1 H), 2.97 (t, $J = 6.7$, 2 H), 2.42 (s, 3 H), 1.88 (m, 2 H), 1.56–1.19 (m, 10 H). ESI-MS m/z (rel intensity) 529 (MH^+ , 78). HRMS (+ESI) calcd for MH^+ , 529.2161; found, 529.2155. HPLC purity: 97.7% (MeOH, 100%), 96.7% (MeOH–H₂O, 90:10).

***N*-(9-(5,11-Dioxo-5*H*-indeno[1,2-*c*]isoquinolin-6(11*H*)-yl)-nonyl)-4-methylbenzenesulfonamide (109).** The crude product was eluted with EtOAc–CHCl₃ (7:3) to afford the desired compound as an orange product (61.3 mg, 80%); mp 159–160 °C. IR (film) 3276, 1769, 1698, 1663, 1610, 1549, 1504, 1427, 1320, 1158, 758 cm⁻¹. ¹H NMR (300 MHz, CDCl₃) δ 8.72 (d, $J = 8.1$ Hz, 1 H), 8.36 (d, $J = 7.4$ Hz, 1 H), 7.75–7.70 (m, 3 H), 7.66 (d, $J = 6.8$ Hz, 1 H), 7.49–7.39 (m, 4 H), 7.32–7.29 (m, 2 H), 4.53 (t, $J = 7.9$ Hz, 2 H), 4.33 (t, $J = 7.1$ Hz, 1 H), 2.96 (m, 2 H), 2.42 (s, 3 H), 1.88 (m, 2 H), 1.51–1.26 (m, 12 H). ESI-MS m/z (rel intensity) 1107 (M_2Na^+ , 18). HRMS (+ESI) calcd for MH^+ , 543.2318; found, 543.2307. Anal. Calcd for C₃₂H₃₄N₂O₄S·0.2H₂O: C, 70.36; H, 6.35; N, 5.13. Found: C, 70.22; H, 6.35; N, 4.97.

***N*-(10-(5,11-Dioxo-5*H*-indeno[1,2-*c*]isoquinolin-6(11*H*)-decyl)-4-methylbenzenesulfonamide (110).** The crude product was eluted with EtOAc–CHCl₃ (10:90) to afford the desired product as a red solid (49.4 mg, 78%); mp 133–135 °C. IR (film) 3263, 1699, 1663, 1611, 1550, 1504, 1428, 1320, 1159, 758 cm⁻¹. ¹H NMR (300 MHz, CDCl₃) δ 8.73 (d, $J = 8.1$ Hz, 1 H), 8.36 (d, $J = 7.4$ Hz, 1 H), 7.76–7.71 (m, 3 H), 7.66 (d, $J = 6.3$ Hz, 1 H), 7.50–7.40 (m, 4 H), 7.32–7.30 (m, 2 H), 4.53 (t, $J = 7.7$ Hz, 2 H), 4.33 (t, $J = 5.9$ Hz, 1 H), 2.97 (q, $J = 6.8$ Hz, 2 H), 2.43 (s, 3 H), 1.92 (m, 2 H), 1.55–1.19 (m, 14 H). APCI-MS m/z (rel intensity) 557 (MH^+ , 100). HRMS (+APCI) calcd for MH^+ , 557.2474; found, 557.2478. HPLC purity: 97.0% (MeOH, 100%), 98.8% (MeOH–H₂O, 90:10).

***N*-(11-(5,11-Dioxo-5*H*-indeno[1,2-*c*]isoquinolin-6(11*H*)-yl)-undecyl)-4-methylbenzenesulfonamide (111).** The crude product was eluted with EtOAc–CHCl₃ (6:4) to afford the desired

compound as an orange solid (45.0 mg, 71.4%); mp 170–172 °C. IR (film) 3289, 1698, 1669, 1609, 1575, 1548, 1505, 1445, 1326, 1160, 760 cm⁻¹. ¹H NMR (300 MHz, CDCl₃) δ 8.72 (d, *J* = 8.0 Hz, 1 H), 8.36 (d, *J* = 8.0 Hz, 1 H), 7.76–7.70 (m, 3 H), 7.65 (d, *J* = 6.4 Hz, 1 H), 7.49–7.40 (m, 4 H), 7.32–7.29 (m, 2 H), 4.53 (t, *J* = 7.5 Hz, 2 H), 4.33 (br s, 1 H), 2.97 (q, *J* = 6.6 Hz, 2 H), 2.43 (s, 3 H), 1.90 (m, 2 H), 1.58–1.23 (m, 16 H). ESI-MS *m/z* (rel intensity) 571 (MH⁺, 100). HRMS (+ESI) calcd for MH⁺, 571.2631; found, 571.2625. HPLC purity: 96.7% (MeOH, 100%), 96.7% (MeOH–H₂O, 95:5).

***N*-(12-(5,11-Dioxo-5*H*-indeno[1,2-*c*]isoquinolin-6(11*H*)-yl)-dodecyl)-4-methylbenzenesulfonamide (112).** The crude product was eluted with EtOAc–CHCl₃ (6:4) to afford the desired compound as an orange solid (55 mg, 73%); mp 108–112 °C. IR (film) 3275, 1698, 1666, 1611, 1550, 1504, 1428, 1320, 1160, 757 cm⁻¹. ¹H NMR (300 MHz, CDCl₃) δ 8.72 (d, *J* = 8.2 Hz, 1 H), 8.36 (d, *J* = 7.0 Hz, 1 H), 7.75–7.63 (m, 4 H), 7.49–7.29 (m, 6 H), 4.53 (t, *J* = 7.3 Hz, 2 H), 4.27 (m, 1 H), 2.96 (q, *J* = 6.7 Hz, 2 H), 2.42 (s, 3 H), 1.90 (m, 2 H), 1.57–1.22 (m, 18 H). ESI-MS *m/z* (rel intensity) 607 (MNa⁺, 30). HRMS (+ESI) calcd for MNa⁺, 607.2607; found, 607.2604. Anal. Calcd for C₃₃H₄₀N₂O₄S: C, 71.89; H, 6.89; N, 4.79. Found: C, 71.49; H, 6.97; N, 4.83.

***N*-(2-(5,11-Dioxo-5*H*-indeno[1,2-*c*]isoquinolin-6(11*H*)-yl)-ethyl)-4-bromobenzenesulfonamide (113).** The crude product was eluted with EtOAc–CHCl₃ (2:8) to afford the desired product as an orange solid (64.2 mg, 82%); mp 260–263 °C. IR (film) 3208, 1707, 1645, 1611, 1551, 1506, 1427, 1324, 1146, 827 cm⁻¹. ¹H NMR (300 MHz, DMSO-*d*₆) δ 8.56 (d, *J* = 8.0 Hz, 1 H), 8.22 (m, 2 H), 7.80–7.69 (m, 4 H), 7.64–7.61 (m, 2 H), 7.56–7.48 (m, 4 H), 4.54 (t, *J* = 6.4 Hz, 2 H), 3.26 (t, *J* = 6.7 Hz, 2 H). ESI-MS *m/z* (rel intensity) 507/509 ([M – H]⁻, 78/100). HRMS (–ESI) calcd for [M – H]⁻, 507.0014; found, 507.0017. HPLC purity: 97.7% (MeOH, 100%), 95.3% (MeOH–H₂O, 90:10).

***N*-(3-(5,11-Dioxo-5*H*-indeno[1,2-*c*]isoquinolin-6(11*H*)-yl)-propyl)-4-bromobenzenesulfonamide (114).** The crude product was eluted with EtOAc–CHCl₃ (9:1) to afford the desired product as an orange solid (40.2 mg, 52%); mp 241–243 °C. IR (film) 3303, 1762, 1696, 1653, 1609, 1549, 1505, 1427, 1325, 1166, 751 cm⁻¹. ¹H NMR (300 MHz, DMSO-*d*₆) δ 8.72 (d, *J* = 8.1 Hz, 1 H), 8.28 (d, *J* = 7.6 Hz, 1 H), 7.79–7.74 (m, 3 H), 7.66–7.39 (m, 7 H), 6.11 (t, *J* = 6.7 Hz, 1 H), 4.67 (t, *J* = 6.0 Hz, 2 H), 3.01 (q, *J* = 6.6 Hz, 2 H), 2.18 (m, 2 H). ESI-MS *m/z* (rel intensity) 523/525 (MH⁺, 100/93). HRMS (+ESI) calcd for MH⁺, 523.0327; found, 523.0335. HPLC purity: 95.4% (MeOH, 100%), 95.7% (MeOH–H₂O, 95:5).

***N*-(4-(5,11-Dioxo-5*H*-indeno[1,2-*c*]isoquinolin-6(11*H*)-yl)-butyl)-4-bromobenzenesulfonamide (115).** The crude product was eluted with EtOAc–CHCl₃ (2:8) to afford the desired product as a red solid (63.7 mg, 84%); mp 176–177 °C. IR (film) 3257, 1698, 1663, 1611, 1576, 1503, 1427, 1332, 1163, 757 cm⁻¹. ¹H NMR (300 MHz, CDCl₃) δ 8.71 (d, *J* = 8.1 Hz, 1 H), 8.32 (d, *J* = 8.0 Hz, 1 H), 7.76–7.70 (m, 3 H), 7.67–7.63 (m, 3 H), 7.49–7.40 (m, 4 H), 4.98 (t, *J* = 6.3 Hz, 1 H), 4.54 (t, *J* = 7.3 Hz, 2 H), 3.14 (q, *J* = 6.4 Hz, 2 H), 1.99 (m, 2 H), 1.80 (m, 2 H). ESI-MS *m/z* (rel intensity) 537/539 (MH⁺, 89/100). HRMS (+ESI) calcd for MH⁺, 537.0484; found, 537.0489. HPLC purity: 99.4% (MeOH, 100%), 98.1% (MeOH–H₂O, 90:10).

***N*-(5-(5,11-Dioxo-5*H*-indeno[1,2-*c*]isoquinolin-6(11*H*)-yl)-pentyl)-4-bromobenzenesulfonamide (116).** The crude product was eluted with EtOAc–CHCl₃ (15:85) to afford the desired product as an orange solid (68.0 mg, 91%); mp 169–171 °C. IR (film) 3271, 1698, 1661, 1611, 1576, 1505, 1428, 1332, 1163, 757 cm⁻¹. ¹H NMR (300 MHz, CDCl₃) δ 8.73 (d, *J* = 8.0 Hz, 1 H), 8.36 (d, *J* = 7.3 Hz, 1 H), 7.74–7.70 (m, 3 H), 7.66–7.61 (m, 3 H), 7.49–7.41 (m, 4 H), 4.73 (t, *J* = 6.0 Hz, 1 H), 4.54 (t, *J* = 7.2 Hz, 2 H), 3.04 (q, *J* = 6.4 Hz, 2 H), 1.92 (m, 2 H), 1.68 (m, 2 H), 1.53 (m, 2 H). ESI-MS *m/z* (rel intensity) 551/553 (MH⁺, 100/98). HRMS (+ESI) calcd for MH⁺, 551.0640; found, 551.0652; HPLC purity: 98.3% (MeOH, 100%), 98.2% (MeOH–H₂O, 90:10).

***N*-(6-(5,11-Dioxo-5*H*-indeno[1,2-*c*]isoquinolin-6(11*H*)-yl)-hexyl)-4-bromobenzenesulfonamide (117).** The crude product was eluted with EtOAc–CHCl₃ (2:8) to afford the desired product as

a red solid (68.5 mg, 93%); mp 188–190 °C. IR (film) 3199, 1760, 1698, 1636, 1610, 1574, 1503, 1458, 1330, 1160, 757 cm⁻¹. ¹H NMR (300 MHz, CDCl₃) δ 8.73 (d, *J* = 8.1 Hz, 1 H), 8.35 (d, *J* = 7.5 Hz, 1 H), 7.76–7.71 (m, 3 H), 7.66–7.64 (m, 3 H), 7.50–7.39 (m, 4 H), 4.74 (t, *J* = 6.2 Hz, 1 H), 4.54 (t, *J* = 7.2 Hz, 2 H), 3.03 (q, *J* = 6.4 Hz, 2 H), 1.89 (m, 2 H), 1.57–1.48 (m, 6 H). ESI-MS *m/z* (rel intensity) 565/567 (MH⁺, 91/100). HRMS (+ESI) calcd for MNa⁺, 587.0616; found, 587.0610. HPLC purity: 96.6% (MeOH, 100%), 98.2% (MeOH–H₂O, 90:10).

***N*-(7-(5,11-Dioxo-5*H*-indeno[1,2-*c*]isoquinolin-6(11*H*)-yl)-heptyl)-4-bromobenzenesulfonamide (118).** The crude product was eluted with EtOAc–CHCl₃ (5:95) to afford the desired product as a red solid (70.5 mg, 96%); mp 160–161 °C. IR (film) 3290, 1699, 1661, 1610, 1550, 1503, 1427, 1320, 1161, 757 cm⁻¹. ¹H NMR (300 MHz, CDCl₃) δ 8.72 (d, *J* = 8.1 Hz, 1 H), 8.36 (d, *J* = 7.7 Hz, 1 H), 7.76–7.70 (m, 3 H), 7.66–7.63 (m, 3 H), 7.50–7.39 (m, 4 H), 4.69 (t, *J* = 6.1 Hz, 1 H), 4.51 (t, *J* = 7.7 Hz, 2 H), 3.01 (q, *J* = 6.7 Hz, 2 H), 1.90 (m, 2 H), 1.53–1.36 (m, 8 H). ESI-MS *m/z* (rel intensity) 579/581 (MH⁺, 92/100). HRMS (+ESI) calcd for MNa⁺, 579.0953; found, 579.0959. HPLC purity: 98.3% (MeOH, 100%), 98.9% (MeOH–H₂O, 90:10).

***N*-(8-(5,11-Dioxo-5*H*-indeno[1,2-*c*]isoquinolin-6(11*H*)-yl)-octyl)-4-bromobenzenesulfonamide (119).** The crude product was eluted with EtOAc–CHCl₃ (6:4) to afford the desired product as an orange solid (67.6 mg, 78%); mp 119–121 °C. IR (film) 3272, 1698, 1662, 1611, 1550, 1504, 1428, 1331, 1163, 757 cm⁻¹. ¹H NMR (300 MHz, CDCl₃) δ 8.73 (d, *J* = 8.1 Hz, 1 H), 8.36 (d, *J* = 8.4 Hz, 1 H), 7.74–7.71 (m, 3 H), 7.67–7.64 (m, 3 H), 7.47–7.43 (m, 4 H), 4.53 (t, *J* = 7.7 Hz, 2 H), 4.43 (t, *J* = 6.4 Hz, 1 H), 3.00 (q, *J* = 6.8 Hz, 2 H), 1.91 (m, 2 H), 1.55–1.20 (m, 10 H). ESI-MS *m/z* (rel intensity) 593/595 (MH⁺, 100/91). HRMS (+ESI) calcd for MH⁺, 593.1110; found, 593.1105. Anal. Calcd for C₃₀H₂₉BrN₂O₄S: C, 60.71; H, 4.92; N, 4.72. Found: C, 60.69; H, 5.01; N, 4.67.

***N*-(9-(5,11-Dioxo-5*H*-indeno[1,2-*c*]isoquinolin-6(11*H*)-yl)-nonyl)-4-bromobenzenesulfonamide (120).** The crude product was eluted with EtOAc–CHCl₃ (6:4) to afford the desired product as an orange solid (52.2 mg, 61%); mp 143–146 °C. IR (film) 3288, 1697, 1662, 1610, 1550, 1504, 1427, 1320, 1162, 757 cm⁻¹. ¹H NMR (300 MHz, CDCl₃) δ 8.72 (d, *J* = 8.1 Hz, 1 H), 8.35 (d, *J* = 8.2 Hz, 1 H), 7.74–7.71 (m, 3 H), 7.66–7.63 (m, 3 H), 7.49–7.40 (m, 4 H), 4.53 (t, *J* = 6.4 Hz, 3 H), 2.99 (q, *J* = 6.8 Hz, 2 H), 1.91 (m, 2 H), 1.58–1.25 (m, 12 H). ESI-MS *m/z* (rel intensity) 607/609 (MH⁺, 88/100). HRMS (+ESI) calcd for MH⁺, 607.1266; found, 607.1263. Anal. Calcd for C₃₁H₃₁BrN₂O₄S: C, 61.28; H, 5.14; N, 4.61. Found: C, 61.22; H, 5.16; N, 4.57.

***N*-(10-(5,11-Dioxo-5*H*-indeno[1,2-*c*]isoquinolin-6(11*H*)-yl)-decyl)-4-bromobenzenesulfonamide (121).** The crude product was eluted with EtOAc–CHCl₃ (6:4) to afford the desired product as an orange solid (65.2 mg, 77%); mp 160–163 °C. IR (film) 3262, 1696, 1658, 1609, 1548, 1503, 1426, 1321, 1158, 753 cm⁻¹. ¹H NMR (500 MHz, CDCl₃) δ 8.72 (d, *J* = 8.0 Hz, 1 H), 8.35 (d, *J* = 8.0 Hz, 1 H), 7.74–7.71 (m, 3 H), 7.66–7.64 (m, 3 H), 7.49–7.40 (m, 4 H), 4.52 (t, *J* = 7.0 Hz, 2 H), 4.40 (m, 1 H), 2.97 (q, *J* = 6.5 Hz, 2 H), 1.91–1.88 (m, 2 H), 1.54–1.22 (m, 14 H). ESI-MS *m/z* (rel intensity) 621/623 (MH⁺, 100/99.8). HRMS (+ESI) calcd for MH⁺, 621.1423; found, 621.1430. Anal. Calcd for C₃₂H₃₃BrN₂O₄S: C, 61.83; H, 5.35; N, 4.51. Found: C, 61.95; H, 5.40; N, 4.71.

***N*-(11-(5,11-Dioxo-5*H*-indeno[1,2-*c*]isoquinolin-6(11*H*)-yl)-undecyl)-4-bromobenzenesulfonamide (122).** The crude product was eluted with EtOAc–CHCl₃ (6:4) to afford the desired product as an orange solid (60.6 mg, 86%); mp 150–153 °C. IR (film) 3310, 1705, 1661, 1608, 1548, 1504, 1422, 1328, 1156, 757 cm⁻¹. ¹H NMR (300 MHz, CDCl₃) δ 8.73 (d, *J* = 8.0 Hz, 1 H), 8.36 (d, *J* = 8.2 Hz, 1 H), 7.75–7.71 (m, 3 H), 7.66–7.61 (m, 3 H), 7.49–7.38 (m, 4 H), 4.54 (t, *J* = 7.5 Hz, 2 H), 4.40 (t, *J* = 6.1 Hz, 1 H), 2.99 (q, *J* = 6.8 Hz, 2 H), 1.90 (m, 2 H), 1.56–1.23 (m, 16 H). ESI-MS *m/z* (rel intensity) 635/637 (MH⁺, 100/92). HRMS (+ESI) calcd for MH⁺, 635.1579; found, 635.1584. Anal. Calcd for C₃₃H₃₅BrN₂O₄S: C, 62.36; H, 5.55; N, 4.41. Found: C, 62.15; H, 5.62; N, 4.44.

***N*-(12-(5,11-Dioxo-5*H*-indeno[1,2-*c*]isoquinolin-6(11*H*)-yl)-dodecyl)-4-bromobenzenesulfonamide (123).** The crude product was eluted with EtOAc–CHCl₃ (6:4) to afford the desired product as an orange solid (65.3 mg, 78%); mp 118–120 °C. IR (film) 3275, 1698, 1664, 1611, 1550, 1504, 1428, 1332, 1164, 757 cm⁻¹. ¹H NMR (300 MHz, CDCl₃) δ 8.72 (d, *J* = 8.3 Hz, 1 H), 8.35 (d, *J* = 8.1 Hz, 1 H), 7.73–7.63 (m, 6 H), 7.49–7.40 (m, 4 H), 4.53 (t, *J* = 7.8 Hz, 2 H), 4.41 (t, *J* = 5.9 Hz, 1 H), 2.99 (q, *J* = 6.7 Hz, 2 H), 1.90–1.87 (m, 2 H), 1.58–1.21 (m, 18 H). ESI-MS *m/z* (rel intensity) 649/651 (MH⁺, 100/80). HRMS (+ESI) calcd for MH⁺, 649.1736; found, 649.1728. Anal. Calcd for C₃₄H₃₇BrN₂O₄S·0.5H₂O: C, 62.00; H, 5.82; N, 4.25. Found: C, 61.71; H, 5.62; N, 4.15.

General Procedure for the Preparation of Indenoisoquinoline Sulfonamides 132–136. Indenoisoquinoline salts 127–131 (50 mg, 0.088–0.102 mmol), prepared previously via the reported literature procedures,⁴⁰ were dissolved in CHCl₃ (15 mL), Et₃N (2 equiv) in CHCl₃ (1 mL) was added, and the solutions were stirred at room temperature for 5 min. Benzenesulfonyl chloride (2 equiv) was added. The mixtures were heated at reflux for 3 h and then washed with satd NaHCO₃ (50 mL) and brine (50 mL). The organic layer was dried over anhydrous Na₂SO₄, filtered, and concentrated, adsorbed onto SiO₂, and purified by flash column chromatography (SiO₂), eluting with EtOAc–CHCl₃ to provide the indenoisoquinoline sulfonamide products 132–136 in high purity.

***N*-(3-(3-Nitro-5,11-dioxo-9-phenyl-5*H*-indeno[1,2-*c*]isoquinolin-6(11*H*)-yl)propyl)benzenesulfonamide (132).** The crude product was eluted with EtOAc–CHCl₃ (2:8) to afford the desired product as an orange solid (22.9 mg, 37%); mp 246–247 °C. IR (film) 3318, 1706, 1658, 1615, 1553, 1501, 1448, 1383, 1336, 1153, 749 cm⁻¹. ¹H NMR (300 MHz, DMSO-*d*₆) δ 8.79 (d, *J* = 2.2 Hz, 1 H), 8.66 (d, *J* = 9.0 Hz, 1 H), 8.54 (dd, *J* = 6.5 and 2.4 Hz, 1 H), 7.89–8.75 (m, 8 H), 7.61–7.45 (m, 6 H), 4.50 (m, 2 H), 3.02 (m, 2 H), 1.97 (m, 2 H). ESI-MS *m/z* (rel intensity) 566 (MH⁺, weak). HRMS (+ESI) calcd for MH⁺, 566.1386; found, 566.1378. HPLC purity: 100% (MeOH, 100%), 99.1% (MeOH–H₂O, 90:10).

***N*-(3-(5,11-Dioxo-5*H*-[1,3]dioxolo[4,5-*g*]indeno[1,2-*c*]isoquinolin-6(11*H*)-yl)propyl)benzenesulfonamide (133).** The crude product was eluted with EtOAc–CHCl₃ (2:8) to afford the desired product as an orange solid (51.3 mg, 81%); mp 225–226 °C. IR (film) 3223, 1700, 1636, 1608, 1562, 1499, 1467, 1329, 1174, 765 cm⁻¹. ¹H NMR (300 MHz, DMSO-*d*₆) δ 7.88–7.76 (m, 4 H), 7.60 (d, *J* = 5.3 Hz, 1 H), 7.58–7.47 (m, 7 H), 6.19 (s, 2 H), 4.43 (t, *J* = 7.3 Hz, 2 H), 2.95 (q, *J* = 6.0 Hz, 2 H), 1.90 (m, 2 H). APCI-MS *m/z* (rel intensity) 489 (MH⁺, 100). HRMS (+APCI) calcd for MNa⁺, 511.0940; found, 511.0949. HPLC purity: 100% (MeOH, 100%), 99.9% (MeOH–H₂O, 90:10).

Methyl 2,3-Dimethoxy-5,11-dioxo-6-(3-(phenylsulfonamido)propyl)-6,11-dihydro-5*H*-indeno[1,2-*c*]isoquinoline-9-carboxylate (134). The crude product was eluted with EtOAc–CHCl₃ (4:6) to afford the desired product as a deep-purple solid (53.7 mg, 88%); mp 249–251 °C. IR (film) 3244, 1727, 1645, 1611, 1554, 1511, 1482, 1321, 1259, 1161, 802, 764 cm⁻¹. ¹H NMR (300 MHz, CDCl₃) δ 8.15–8.12 (m, 2 H), 8.07 (s, 1 H), 7.92 (d, *J* = 7.1 Hz, 2 H), 7.63 (s, 1 H), 7.56–7.45 (m, 4 H), 6.04 (t, *J* = 6.4 Hz, 1 H), 4.65 (t, *J* = 6.1 Hz, 2 H), 4.07 (s, 3 H), 4.03 (s, 3 H), 3.97 (s, 3 H), 3.08 (q, *J* = 6.2 Hz, 2 H), 2.12 (m, 2 H). APCI-MS *m/z* (rel intensity) 563 (MH⁺, 100). HRMS (+APCI) calcd for MNa⁺, 585.1308; found, 585.1302. HPLC purity: 100% (MeOH, 100%), 99.9% (MeOH–H₂O, 90:10).

***N*-(3-(3-Nitro-5,11-dioxo-5*H*-indeno[1,2-*c*]isoquinolin-6(11*H*)-yl)propyl)benzenesulfonamide (135).** The crude product was eluted with EtOAc–CHCl₃ (2:8) to afford the desired product as an orange solid (28.6 mg, 46%); mp 258–259 °C. IR (film) 3214, 1699, 1656, 1613, 1553, 1503, 1453, 1423, 1381, 1324, 1259, 1158, 802, 746 cm⁻¹. ¹H NMR (300 MHz, DMSO-*d*₆) δ 8.88 (d, *J* = 2.4 Hz, 1 H), 8.74 (d, *J* = 8.9 Hz, 1 H), 8.60 (dd, *J* = 6.5 and 2.4 Hz, 1 H), 7.91 (t, *J* = 8.0 Hz, 2 H), 7.82 (dd, *J* = 6.7 and 1.5 Hz, 2 H), 7.66–7.57 (m, 6 H), 4.51 (t, *J* = 8.0 Hz, 2 H), 3.01 (q, *J* = 6.2 Hz, 2 H), 1.96 (m, 2 H). APCI-MS *m/z* (rel intensity) 490 (MH⁺, 100). HRMS (+APCI) calcd for MH⁺, 490.1073; found, 490.1070. HPLC purity: 97.1% (MeOH, 100%), 100% (MeOH–H₂O, 90:10).

***N*-(3-(2,3-Dimethoxy-5,11-dioxo-5*H*-indeno[1,2-*c*]isoquinolin-6(11*H*)-yl)propyl)benzenesulfonamide (136).** The crude product was eluted with EtOAc–CHCl₃ (4:6) to afford the desired product as an orange solid (58.9 mg, 94%); mp 249–250 °C. IR (film) 3166, 1701, 1626, 1612, 1589, 1554, 1513, 1478, 1426, 1335, 1260, 1171, 1093, 1021, 789 cm⁻¹. ¹H NMR (300 MHz, CDCl₃) δ 8.12 (s, 1 H), 7.91 (dd, *J* = 6.8 and 1.6 Hz, 2 H), 7.64 (s, 1 H), 7.60 (d, *J* = 6.6 Hz, 1 H), 7.52–7.37 (m, 6 H), 6.12 (t, *J* = 6.9 Hz, 1 H), 4.65 (t, *J* = 5.9 Hz, 2 H), 4.07 (s, 3 H), 4.03 (s, 3 H), 3.05 (q, *J* = 6.3 Hz, 2 H), 2.13 (m, 2 H). ESI-MS *m/z* (rel intensity) 505 (MH⁺, 100). HRMS (+ESI) calcd for MH⁺, 505.1433; found, 505.1423. HPLC purity: 100% (MeOH, 100%), 100% (MeOH–H₂O, 90:10).

General Procedure for the Preparation of Bisindenoisoquinolines 140–142. Diamines 137–139 (100 mg, 1 equiv) were dissolved in CHCl₃ (10 mL) and added to a solution of lactone 11 (2 equiv) in CHCl₃ (20 mL). The mixtures were stirred at reflux for 16 h and then concentrated, adsorbed onto SiO₂, and purified with flash column chromatography (SiO₂), eluting with CHCl₃ to afford the products 140–142 as orange or red solids.

6,6'-(Decane-1,10-diyl)bis(5*H*-indeno[1,2-*c*]isoquinoline-5,11[6*H*]-dione) (140). The general procedure provided the product as an orange solid (223 mg, 64%); mp 201–202 °C. IR (film) 1762, 1657, 1609 cm⁻¹. ¹H NMR (300 MHz, CDCl₃) δ 8.72 (d, *J* = 8.1 Hz, 2 H), 8.35 (d, *J* = 8.2 Hz, 2 H), 7.75 (d, *J* = 8.3 Hz, 2 H), 7.64 (d, *J* = 6.4 Hz, 2 H), 7.49–7.39 (m, 8 H), 4.53 (t, *J* = 7.9 Hz, 4 H), 1.90 (m, 4 H), 1.57 (m, 4 H), 1.54–1.38 (m, 8 H). ESI-MS *m/z* (rel intensity) 633 (MH⁺, 57). HRMS (+ESI) calcd for MH⁺, 633.2753; found, 633.2763. Anal. Calcd for C₄₂H₃₆N₂O₄: C, 79.72; H, 5.73; N, 4.43. Found: C, 79.53; H, 5.76; N, 4.39.

6,6'-(Undecane-1,11-diyl)bis(5*H*-indeno[1,2-*c*]isoquinoline-5,11[6*H*]-dione) (141). The general procedure provided the product as an orange solid (223 mg, 64%); mp 201–202 °C. IR (film) 1764, 1736, 1702, 1655 cm⁻¹. ¹H NMR (300 MHz, CDCl₃) δ 8.71 (d, *J* = 8.1 Hz, 2 H), 8.35 (d, *J* = 7.7 Hz, 2 H), 7.82 (d, *J* = 8.2 Hz, 2 H), 7.64 (d, *J* = 6.5 Hz, 2 H), 7.48–7.38 (m, 8 H), 4.52 (t, *J* = 8.1 Hz, 4 H), 1.92 (m, 4 H), 1.58 (m, 4 H), 1.41–1.33 (m, 10 H). ESI-MS *m/z* (rel intensity) 647 (MH⁺, 100). HRMS (+ESI) calcd for MH⁺, 647.2910; found, 647.2908. Anal. Calcd for C₄₃H₃₈N₂O₄: C, 79.85; H, 5.92; N, 4.33. Found: C, 79.80; H, 5.99; N, 4.29.

6,6'-(Dodecane-1,12-diyl)bis(5*H*-indeno[1,2-*c*]isoquinoline-5,11[6*H*]-dione) (142). The general procedure provided the product as a red solid (135 mg, 82%); mp 226–228 °C. IR (film) 1694, 1660, 1609 cm⁻¹. ¹H NMR (300 MHz, CDCl₃) δ 8.71 (d, *J* = 8.0 Hz, 2 H), 8.35 (d, *J* = 8.1 Hz, 2 H), 7.74 (t, *J* = 7.5 Hz, 2 H), 7.64 (d, *J* = 6.9 Hz, 2 H), 7.48–7.37 (m, 8 H), 4.52 (t, *J* = 7.9 Hz, 4 H), 1.90 (m, 4 H), 1.53 (m, 4 H), 1.40–1.31 (m, 12 H). ESI-MS *m/z* (rel intensity) 661 (MH⁺, 100). HRMS (+ESI) calcd for MH⁺, 661.3066; found, 661.3054. HPLC purity: 99.7% (CH₃CN, 100%), 97.0% (CH₃CN–H₂O, 95:5).

Bis-1,3-[(5,6-dihydro-5,11-diketo-11*H*-indeno[1,2-*c*]isoquinoline)-(6-propyl-*tert*-BOC-amino)]propane (144).³⁷ Tetramine 143 (100 mg, 0.53 mmol) was diluted in CHCl₃ (10 mL) and added to a solution of lactone 11 (276 mg, 1.12 mmol) in CHCl₃ (40 mL). The reaction mixture was stirred at reflux for 72 h. Et₃N (270 mg, 2.66 mmol) and Boc₂O (360 mg, 1.65 mmol) were then added to the cooled mixture, and stirring continued at room temperature for 16 h. The mixture was concentrated, adsorbed onto SiO₂, and purified with flash column chromatography (SiO₂), eluting with EtOAc–hexane (2:8) and then with MeOH–CHCl₃ (3:97) to provide the product as an orange solid (352 mg, 78%); mp 84–86 °C (lit.³⁷ 86–88 °C). ¹H NMR (CDCl₃) δ 8.63 (d, *J* = 7.9 Hz, 2 H), 8.24 (d, *J* = 7.6 Hz, 2 H), 7.65 (t, *J* = 7.3 Hz, 2 H), 7.55 (d, *J* = 6.9 Hz, 2 H), 7.41–7.30 (m, 8 H), 4.49 (br s, 4 H), 3.44 (br s, 4 H), 3.27 (t, *J* = 6.3 Hz, 4 H), 2.08 (br s, 4 H), 1.86 (br s, 2 H), 1.41 (br s, 18 H).

Bis-1,3-[(5,6-dihydro-5,11-diketo-11*H*-indeno[1,2-*c*]isoquinoline)-(6-propylamino)]propane Bis(trifluoroacetate) (145).³⁷ Boc-protected bis(indenoisoquinoline) 144 (352 mg, 0.41 mmol) was diluted in CF₃COOH (30 mL), and the mixture was stirred at room temperature for 2 h. The reaction mixture was concentrated, and the resultant solid was triturated with chloroform and filtered to provide the product as an orange solid (247 mg, 93%);

mp 224–226 °C (lit.³⁷ 225–227 °C). ¹H NMR (DMSO-*d*₆) δ 8.59–8.57 (m, 6 H), 8.22 (d, *J* = 8.1 Hz, 2 H), 7.86–7.78 (m, 4 H), 7.62–7.49 (m, 8 H), 4.60 (t, *J* = 6.4 Hz, 4 H), 3.08 (br s, 4 H), 2.96 (br s, 4 H), 2.15 (br s, 4 H), 1.90 (m, 2 H). HPLC purity: 97.7% (MeOH–H₂O, 80:20), 97.6% (MeOH–H₂O, 70:30).

Biological Tests. *Topoisomerase I-Mediated DNA Cleavage Reactions.* Human recombinant Top1 was purified from baculovirus as previously described.⁴⁵ DNA cleavage reactions were prepared as previously reported with the exception of the DNA substrate.⁴⁶ Briefly, a 117-bp DNA oligonucleotide (Integrated DNA Technologies) encompassing the previously identified Top1 cleavage sites in the 161-bp fragment from pBluescript SK(–) phagemid DNA was employed. This 117-bp oligonucleotide contains a single 5'-cytosine overhang, which was 3'-end-labeled by fill-in reaction with [α -³²P]dGTP in React 2 buffer (50 mM Tris-HCl, pH 8.0, 100 mM MgCl₂, 50 mM NaCl) with 0.5 unit of DNA polymerase I (Klenow fragment, New England BioLabs). Unincorporated [³²P]dGTP was removed using mini Quick Spin DNA columns (Roche, Indianapolis, IN), and the eluate containing the 3'-end-labeled DNA substrate was collected. Approximately 2 nM radiolabeled DNA substrate was incubated with recombinant Top1 in 20 μ L of reaction buffer [10 mM Tris-HCl (pH 7.5), 50 mM KCl, 5 mM MgCl₂, 0.1 mM EDTA, and 15 μ g/mL BSA] at 25 °C for 20 min in the presence of various concentrations of compounds. The reactions were terminated by adding SDS (0.5% final concentration) followed by the addition of two volumes of loading dye (80% formamide, 10 mM sodium hydroxide, 1 mM sodium EDTA, 0.1% xylene cyanol, and 0.1% bromophenol blue). Aliquots of each reaction mixture were subjected to 20% denaturing PAGE. Gels were dried and visualized by using a phosphorimager and ImageQuant software (Molecular Dynamics). For simplicity, cleavage sites were numbered as previously described in the 161-bp fragment.⁴⁵

Gel-Based Assay Measuring the Inhibition of Recombinant Tdp1. A 5'-[³²P]-labeled single-stranded DNA oligonucleotide containing a 3'-phosphotyrosine (N14Y) was generated as described by Dexheimer et al.³⁴ The DNA substrate was then incubated with 5 pM recombinant Tdp1 in the absence or presence of inhibitor for 15 min at room temperature in a buffer containing 50 mM Tris HCl, pH 7.5, 80 mM KCl, 2 mM EDTA, 1 mM DTT, 40 μ g/mL BSA, and 0.01% Tween-20. Reactions were terminated by the addition of 1 volume of gel loading buffer [99.5% (v/v) formamide, 5 mM EDTA, 0.01% (w/v) xylene cyanol, and 0.01% (w/v) bromophenol blue]. Samples were subjected to a 16% denaturing PAGE and gels were exposed after drying to a PhosphorImager screen (GE Healthcare). Gel images were scanned using a Typhoon 8600 (GE Healthcare), and densitometric analyses were performed using the ImageQuant software (GE Healthcare).

*Gel-Based Assay Measuring the Inhibition of Endogenous Human Tdp1 in Whole Cell Extract.*¹⁷ DT40 knockout cells (1 \times 10⁷) for chicken Tdp1 and complemented with human Tdp1 were collected, washed, and centrifuged. Cell pellet was then resuspended with 100 μ L of CellLytic M cell lysis reagent (SIGMA-Aldrich C2978). After 15 min, the lysate was centrifuged at a 12000g for 10 min, and the supernatant was transferred to a new tube. Protein concentration was determined using a nanodrop spectrophotometer (Invitrogen), and the whole cell extract was stored at –80 °C. The 5'-[³²P]-labeled single-stranded N14Y DNA oligonucleotide containing a 3'-phosphotyrosine (see above) was incubated with 1–5 μ g/mL of whole cell extract in the absence or presence of inhibitor for 15 min at room temperature in the same assay buffer used for recombinant Tdp1 (see section above). Reactions were then treated similarly to the recombinant enzyme containing samples (see section above).

All compounds were first tested in gel-based assays for Tdp1 inhibition using recombinant (rec) human Tdp1, and only the active compounds were tested for human Tdp1 inhibition in whole cell extract (WCE). Furamidine (Figure 2) was included in all experiments as positive control.

Determination of the Mechanism of Inhibition of Compound 70.

Mechanistic characterization of compound 70 was carried out using a FRET assay employing a custom designed substrate (Birmingham et al. manuscript in preparation). The assay followed the real-time observation of reaction time-course data, permitting an accurate measure of the reaction rate in the presence of an inhibitor. The mechanism of inhibition of 70 was observed by measuring the rate of the Tdp1 catalyzed reaction under a matrix of varying substrate and inhibitor concentrations. In the assay, Tdp1 FRET substrate was present as a dilution series ranging from 2.25 to 0.035 μ M over eight 2-fold steps. Compound 70 was present at three concentrations equaling 0.33 \times IC₅₀, 1.0 \times IC₅₀, and 3.0 \times IC₅₀. A “no inhibitor” sample was also included to allow measurement of the rate of reaction in the absence of inhibition.

Immediately prior to executing the assay, stocks of Tdp1 enzyme, Tdp1 FRET substrate and compound 70 were created at 3 \times their final desired assay concentrations. Five μ L of compound 70 stock dilutions were combined with 5 μ L of a 1.5 nM Tdp1 stock in appropriate wells in a low volume 384-well plate (Greiner 784900, Greiner, Monroe, NC) and allowed to incubate on ice for 1 h to ensure complete binding equilibrium. After incubation, 5 μ L of the 3 \times Tdp1 FRET substrate dilution series was added to the plate to initiate the reaction. The assay plate was placed in a Tecan Safire plate reader (Tecan US, Durham, NC) and time-course data observed for 1 h at excitation and emission wavelengths of 525 nm (bandwidth = 5) and 545 nm (bandwidth = 5) respectively for all wells. The final assay volume was 15 μ L, with Tdp1 present at a final fixed concentration of 500 pM for all wells. Experimental data was plotted as reaction rate versus substrate concentration for all inhibitor concentrations and analyzed using models for competitive, noncompetitive (pure and mixed) and uncompetitive inhibition (eqs A–D, respectively) using GraphPad Prism (Graphpad, La Jolla, CA). To identify the most appropriate mechanistic model describing the inhibition data, Akaike's Information Criterion (Akaike, H., 1973) was used. Information theory and an extension of the maximum likelihood principle in ref 47 was employed.

Equations. A. Competitive Inhibition.

$$v = \frac{V_{\max}[S]}{[S] + K_m \left(1 + \frac{[I]}{K_i}\right)}$$

Where V_{\max} is maximum reaction velocity, $[S]$ is the substrate concentration, K_m is the Michaelis constant, and K_i is the inhibition constant.

B. Pure Noncompetitive Inhibition.

$$v = \frac{V_{\max}[S]}{([S] + K_m) \left(1 + \frac{[I]}{K_i}\right)}$$

Where K_i is the inhibition constant in the presence or absence of substrate.

C. Mixed Noncompetitive Inhibition.

$$v = \frac{V_{\max}[S]}{[S] \left(1 + \frac{[I]}{K_{ies}}\right) + K_m \left(1 + \frac{[I]}{K_{ie}}\right)}$$

Where K_{ie} is the inhibition constant for binding to the enzyme in the absence of substrate, and K_{ies} the inhibition constant for binding to the ES complex.

D. Uncompetitive Inhibition.

$$v = \frac{V_{\max}[S]}{[S] \left(1 + \frac{[I]}{K_{ies}}\right) + K_m}$$

Where K_{ies} is the inhibition constant for binding to the ES complex.

Surface Plasmon Resonance Analysis. Binding experiments were performed on a Biacore T100 instrument (GE, Piscataway, NJ). Tdp1 was amine coupled to a CMS sensor chip (GE Healthcare, Piscataway NJ). Coupling reagents [*N*-ethyl-*N'*-(3-

dimethylaminopropyl)carbodiimide] (EDC), *N*-hydroxysuccinimide (NHS), and ethanolamine were purchased from GE Healthcare (Piscataway, NJ). Neutravidin was obtained from Pierce. To protect the amine groups within the active site from modification, Tdp1 was bound with a 14-base oligonucleotide before coupling to the surface. Specifically, 1 μ M Tdp1 was incubated with 2 μ M of a 14-base oligonucleotide containing a phosphate group at the 3' end (GATCTAAAAGACTT) in 10 mM sodium acetate pH 4.5 for 20 min. The CMS chip surface was activated for 7 min with 0.1 M NHS and 0.4 M EDC at a flow rate of 20 μ L/min and Tdp1-oligonucleotide mixture was injected until approximately 4000 RU's was attached. Activated amine groups were quenched with an injection of 1 M solution of ethanolamine pH 8.0 for 7 min. Any bound oligonucleotide was removed by washing the surface with 1 M NaCl. A reference surface was prepared in the same manner without coupling of Tdp1. Compound 70 was diluted into running buffer [10 mM Hepes, 150 mM NaCl, 0.01% tween 20 (v/v), 5% DMSO (v/v) pH 7.5] and injected over all flow cells at 30 μ L/min at 25 °C. Following compound injections, the surface was regenerated with a 30 s injection 1 M NaCl, a 30 s injection of 50% DMSO (v/v), and a 30 s running buffer injection. Each cycle of compound injection was followed by buffer cycle for referencing purposes. A DMSO calibration curve was included to correct for refractive index mismatches between the running buffer and compound dilution series.

AUTHOR INFORMATION

Corresponding Author

*Phone: 765-494-1465. Fax: 765-494-6790. E-mail: cushman@purdue.edu.

Notes

The authors declare no competing financial interest.

ACKNOWLEDGMENTS

This work was made possible by the National Institutes of Health (NIH) through support with Research Grant UO1 CA89566, and by a Purdue Research Foundation Grant. This research was also supported in part by the Intramural Research Program of the NIH, National Cancer Institute, Center for Cancer Research. This project has been funded in part with federal funds from the National Cancer Institute, National Institutes of Health, under Contract no. HHSN261200800001E. The content of this publication does not necessarily reflect the views or policies of the Department of Health and Human Services, nor does mention of trade names, commercial products, or organizations imply endorsement by the U.S. Government.

ABBREVIATIONS USED

APCI-MS, atmospheric-pressure chemical ionization mass spectrometry; CI/EI-MS, chemical ionization/electron impact mass spectrometry; CPT, camptothecin; DMAP, 4-dimethylaminopyridine; DMSO-*d*₆, dimethyl-*d*₆ sulfoxide; ESI-MS, electrospray ionization mass spectrometry; HRMS, high resolution mass spectrometry; PTSA, *p*-toluenesulfonic acid; SCAN1, spinocerebellar ataxia with axonal neuropathy; Tdp1, tyrosyl-DNA phosphodiesterase I; TFA, trifluoroacetic acid; Top1, topoisomerase type I; TsCl, *p*-toluenesulfonyl chloride

REFERENCES

- (1) Wang, J. C. DNA Topoisomerases. *Annu. Rev. Biochem.* **1996**, *65*, 635–692.
- (2) Pommier, Y. Topoisomerase I Inhibitors: Camptothecins and Beyond. *Nature Rev. Cancer* **2006**, *6*, 789–802.
- (3) Champoux, J. J. DNA Topoisomerases: Structure, Function, and Mechanism. *Annu. Rev. Biochem.* **2001**, *70*, 369–413.

- (4) Pourquier, P.; Pommier, Y. Topoisomerase I-Mediated DNA Damage. *Adv. Cancer Res.* **2001**, *80*, 189–216.

- (5) Pommier, Y.; Redon, C.; Rao, V. A.; Seiler, J. A.; Sordet, O.; Takemura, H.; Antony, S.; Meng, L.; Liao, Z.; Kohlhagen, G.; Zhang, H.; Kohn, K. W. Repair of and Checkpoint Response to Topoisomerase I-mediated DNA Damage. *Mutat. Res.* **2003**, *532*, 173–203.

- (6) Pommier, Y.; Marchand, C. Interfacial Inhibitors: Targeting Macromolecular Complexes. *Nature Rev. Drug Discovery* **2012**, *11*, 25–36.

- (7) Chen, A. Y.; Liu, L. F. DNA Topoisomerases: Essential Enzymes and Lethal Targets. *Annu. Rev. Pharmacol. Toxicol.* **1994**, *34*, 191–218.

- (8) Gupta, M.; Fujimori, A.; Pommier, Y. Eukaryotic DNA Topoisomerases I. *Biochim. Biophys. Acta* **1995**, *1262*, 1–14.

- (9) Pommier, Y.; Pourquier, P.; Urasaki, Y.; Wu, J.; Laco, G. S. Topoisomerase I Inhibitors: Selectivity and Cellular Resistance. *Drug Resist. Updat.* **1999**, *2*, 307–318.

- (10) Pourquier, P.; Pilon, A. A.; Kohlhagen, G.; Mazumder, A.; Sharma, A.; Pommier, Y. Trapping of Mammalian Topoisomerase I and Recombinations Induced by Damaged DNA Containing Nicks or Gaps. Importance of DNA End Phosphorylation and Camptothecin Effects. *J. Biol. Chem.* **1997**, *272*, 26441–26447.

- (11) Pourquier, P.; Ueng, L.; Kohlhagen, G.; Mazumder, A.; Gupta, M.; Kohn, K. W.; Pommier, Y. Effects of Uracil Incorporation, DNA Mismatches, and Abasic Sites on Cleavage and Religation Activities of Mammalian Topoisomerase I. *J. Biol. Chem.* **1997**, *272*, 7792–7796.

- (12) Dexheimer, T. S.; Antony, S.; Marchand, C.; Pommier, Y. Tyrosyl-DNA Phosphodiesterase as a Target for Anticancer Therapy. *Anticancer Agents Med. Chem* **2008**, *8*, 381–389.

- (13) Yang, S. W.; Burgin, A. B., Jr.; Huizenga, B. N.; Robertson, C. A.; Yao, K. C.; Nash, H. A. An Eukaryotic Enzyme that can Disjoin Dead-End Covalent Complexes between DNA and Type I Topoisomerases. *Proc. Natl. Acad. Sci. U.S.A.* **1996**, *93*, 11534–11539.

- (14) Takashima, H.; Boerkoel, C. F.; John, J.; Saifi, G. M.; Salih, M. A. M.; Armstrong, D.; Mao, Y.; Quiocho, F. A.; Roa, B. B.; Nakagawa, M.; Stockton, D. W.; Lupski, J. R. Mutation of Tdp1, Encoding a Topoisomerase I-Dependent DNA Damage Repair Enzyme, in Spinocerebellar Ataxia with Axonal Neuropathy. *Nature Genet.* **2002**, *32*, 267–272.

- (15) Zhou, T.; Lee, J. W.; Tatavarthi, H.; Lupski, J. R.; Valerie, K.; Povirk, L. F. Deficiency in 3'-Phosphoglycolate Processing in Human Cells with a Hereditary Mutation in Tyrosyl-DNA phosphodiesterase (Tdp1). *Nucleic Acids Res.* **2005**, *33*, 289–297.

- (16) Barthelmes, H. U.; Habermeyer, M.; Christensen, M. O.; Mielke, C.; Interthal, H.; Pouliot, J. J.; Boege, F.; Marko, D. Tdp1 Overexpression in Human Cells Counteracts DNA Damage Mediated by Topoisomerases I and II. *J. Biol. Chem.* **2004**, *279*, 55618–55625.

- (17) Murai, J.; Huang, S. N.; Das, B. B.; Dexheimer, T. S.; Takeda, S.; Pommier, Y. Tyrosyl-DNA phosphodiesterase 1 (TDP1) Repairs DNA Damages Induced by Topoisomerases I and II, and Base Alkylation in Vertebrate Cells. *J. Biol. Chem.* **2012**, *287*, 12848–12857.

- (18) Marchand, C.; Lea, W. A.; Jadhav, A.; Dexheimer, T. S.; Austin, C. P.; Inglese, I.; Pommier, Y.; Simeonov, A. Identification of Phosphotyrosine Mimetic Inhibitors of Human Tyrosyl-DNA Phosphodiesterase I by a Novel AlphaScreen High-Throughput Assay. *Mol. Cancer Ther.* **2009**, *8*, 240–248.

- (19) Interthal, H.; Pouliot, J. J.; Champoux, J. J. The Tyrosyl-DNA Phosphodiesterase Tdp1 is a Member of the Phospholipase D Superfamily. *Proc. Natl. Acad. Sci. U.S.A.* **2001**, *98*, 12009–12014.

- (20) Davies, D. R.; Interthal, H.; Champoux, J. J.; Hol, W. G. J. The Crystal Structure of Human Tyrosyl-DNA Phosphodiesterase, Tdp1. *Structure* **2002**, *10*, 237–248.

- (21) Davies, D. R.; Interthal, H.; Champoux, J. J.; Hol, W. G. J. Insights into Substrate Binding and Catalytic Mechanism of Human Tyrosyl-DNA Phosphodiesterase (Tdp1) from Vanadate and Tungstate-Inhibited Structures. *J. Mol. Biol.* **2002**, *324*, 917–932.

- (22) Davies, D. R.; Interthal, H.; Champoux, J. J.; Hol, W. G. J. Crystal Structure of a Transition State Mimic for Tdp1 Assembled

From Vanadate, DNA, and a Topoisomerase I-derived Peptide. *Chem. Biol.* **2003**, *10*, 139–147.

(23) Interthal, H.; Chen, H. J.; Kehl-Fie, T. E.; Zotzmann, J.; Leppard, J. B.; Champoux, J. J. SCAN1 Mutant Tdp1 Accumulates the Enzyme–DNA Intermediate and Causes Camptothecin Hypersensitivity. *EMBO J.* **2005**, *24*, 2224–2233.

(24) Redinbo, M. R.; Stewart, L.; Kuhn, P.; Champoux, J. J.; Hol, W. G. J. Crystal Structures of Human Topoisomerase I in Covalent and Noncovalent Complexes with DNA. *Science* **1998**, *279*, 1504–1513.

(25) Debéthune, L.; Kohlhagen, G.; Grandas, A.; Pommier, Y. Processing of Nucleopeptides Mimicking the Topoisomerase I–DNA Covalent Complex by Tyrosyl-DNA Phosphodiesterase. *Nucleic Acids Res.* **2002**, *30*, 1198–1204.

(26) Interthal, H.; Champoux, J. J. Effects of DNA and Protein Size on Substrate Cleavage by Human Tyrosyl-DNA Phosphodiesterase I. *Biochem. J.* **2011**, *436*, 559–566.

(27) Pouliot, J. J.; Robertson, C. A.; Nash, H. A. Pathways for Repair of Topoisomerase I Covalent Complexes in *Saccharomyces cerevisiae*. *Genes Cells* **2001**, *6*, 677–687.

(28) Raymond, A. C.; Staker, B. L.; Burgin, A. B., Jr. Substrate Specificity of Tyrosyl-DNA Phosphodiesterase I (Tdp1). *J. Biol. Chem.* **2005**, *280*, 22029–22035.

(29) El-Khamisy, S. F.; Saifi, G. M.; Weinfeld, M.; Johansson, F.; Helleday, T.; Lupski, J. R.; Caldecott, K. W. Defective DNA Single-Strand Break Repair in Spinocerebellar Ataxia with Axonal Neuroathy-1. *Nature* **2005**, *434*, 108–113.

(30) Miao, Z. H.; Agama, K.; Sordet, O.; Povirk, L.; Kohn, K. W.; Pommier, Y. Hereditary Ataxia SCAN1 Cells are Defective for the Repair of Transcription-Dependent Topoisomerase I Cleavage Complexes. *DNA Repair* **2006**, *5*, 1489–1494.

(31) Nivens, M. C.; Felder, T.; Galloway, A. H.; Pena, M. M. O.; Pouliot, J. J.; Spencer, H. T. Engineered Resistance to Camptothecin and Antifolates by Retroviral Coexpression of Tyrosyl DNA Phosphodiesterase-I and Thymidylate Synthase. *Cancer Chemother. Pharmacol.* **2004**, *53*, 107–115.

(32) Liao, Z.; Thibaut, L.; Jobson, A.; Pommier, Y. Inhibition of Human Tyrosyl-DNA Phosphodiesterase by Aminoglycoside Antibiotics and Ribosome Inhibitors. *Mol. Pharmacol.* **2006**, *70*, 366–372.

(33) Antony, S.; Marchand, C.; Stephen, A. G.; Thibaut, L.; Agama, K. K.; Fisher, R. J.; Pommier, Y. Novel High-Throughput Electrochemiluminescent Assay for Identification of Human Tyrosyl-DNA Phosphodiesterase (Tdp1) Inhibitors and Characterization of Furamidine (NSC 305831) as an Inhibitor of Tdp1. *Nucleic Acids Res.* **2007**, *35*, 4474–4484.

(34) Dexheimer, T. S.; Gediya, L. K.; Stephen, A. G.; Weidlich, I.; Antony, S.; Marchand, C.; Interthal, H.; Nicklaus, M.; Fisher, R. J.; Njar, V. C.; Pommier, Y. 4-Pregnen-21-ol-3,20-dione-21-(4-bromobenzenesulfonate) (NSC 88915) and Related Novel Steroid Derivatives as Tyrosyl-DNA Phosphodiesterase (Tdp1) Inhibitors. *J. Med. Chem.* **2009**, *52*, 7122–7131.

(35) Morrell, A.; Placzek, M. S.; Steffen, J. D.; Antony, S.; Agama, K.; Pommier, Y.; Cushman, M. Investigation of the Lactam Side Chain Length Necessary for Optimal Indenoisoquinoline Topoisomerase I Inhibition and Cytotoxicity in Human Cancer Cell Cultures. *J. Med. Chem.* **2007**, *50*, 2040–2048.

(36) Davies, D. R.; Interthal, H.; Champoux, J. J.; Hol, W. G. J. Explorations of Peptide and Oligonucleotide Binding Sites of Tyrosyl-DNA Phosphodiesterase Using Vanadate Complexes. *J. Med. Chem.* **2004**, *47*, 829–837.

(37) Nagarajan, M.; Morrell, A.; Antony, S.; Kohlhagen, G.; Agama, K.; Pommier, Y.; Ragazzon, P. A.; Garbett, N. C.; Chaires, J. B.; Hollingshead, M.; Cushman, M. Synthesis and Biological Evaluation of Bisindenoisoquinolines as Topoisomerase I Inhibitors. *J. Med. Chem.* **2006**, *49*, 5129–5140.

(38) Morrell, A.; Antony, S.; Kohlhagen, G.; Pommier, Y.; Cushman, M. Synthesis of Benz[*d*]indeno[1,2-*b*]pyran-5,11-diones: Versatile Intermediates for the Design and Synthesis of Topoisomerase I Inhibitors. *Bioorg. Med. Chem. Lett.* **2006**, *16*, 1846–1849.

(39) Conrow, R. E.; Dean, W. D. Diazidomethane Explosion. *Org. Process Res. Dev.* **2008**, *12*, 1285–1286.

(40) Morrell, A.; Placzek, M.; Parmley, S.; Grella, B.; Antony, S.; Pommier, Y.; Cushman, M. Optimization of the Indenone Ring of Indenoisoquinoline Topoisomerase I Inhibitors. *J. Med. Chem.* **2007**, *50*, 4388–4404.

(41) Dexheimer, T. S.; Pommier, Y. DNA Cleavage Assay for the Identification of Topoisomerase I Inhibitors. *Nature Protoc.* **2008**, *3*, 1736–1750.

(42) Cushman, M.; Jayaraman, M.; Vroman, J. A.; Fukunaga, A. K.; Fox, B. M.; Kohlhagen, G.; Strumberg, D.; Pommier, Y. Synthesis of New Indeno[1,2-*c*]isoquinolines: Cytotoxic Non-Camptothecin Topoisomerase I Inhibitors. *J. Med. Chem.* **2000**, *43*, 3688–3698.

(43) Strumberg, D.; Pommier, Y.; Paull, K.; Jayaraman, M.; Nagafuji, P.; Cushman, M. Synthesis of Cytotoxic Indenoisoquinoline Topoisomerase I Poisons. *J. Med. Chem.* **1999**, *42*, 446–457.

(44) Ahn, G.; Lansiaux, A.; Goossens, J.; Bailly, C.; Baldeyrou, B.; Schifano-Faux, N.; Grandclaude, P.; Couture, A.; Ryckebusch, A. Indeno[1,2-*c*]isoquinolin-5,11-diones Conjugated to Amino Acids: Synthesis, Cytotoxicity, DNA Interaction, and Topoisomerase II Inhibition Properties. *Bioorg. Med. Chem.* **2010**, *18*, 8119–8133.

(45) Pourquier, P.; Ueng, L.-M.; Fertala, J.; Wang, D.; Park, H.-J.; Essigmann, J. M.; Bjornsti, M.-A.; Pommier, Y. Induction of Reversible Complexes between Eukaryotic DNA Topoisomerase I and DNA containing Oxidative Base Damages. 7,8-Dihydro-8-Oxoguanine and 5-Hydroxycytosine. *J. Biol. Chem.* **1999**, *274*, 8516–8523.

(46) Antony, S.; Agama, K. K.; Miao, Z. H.; Takagi, K.; Wright, M. H.; Robles, A. I.; Varticovski, L.; Nagarajan, M.; Morrell, A.; Cushman, M.; Pommier, Y. Novel Indenoisoquinolines NSC 725776 and NSC 724998 Produce Persistent Topoisomerase I Cleavage Complexes and Overcome Multidrug Resistance. *Cancer Res.* **2007**, *67*, 10397–10405.

(47) *Second International Symposium on Information Theory*; Petrov, B. N., Csaki, F., Eds.; Akademiai Kiado: Budapest, 1973.